UNIVERSITY OF TWENTE.

Faculty of Geo-Information Science
and Earth Observation

Optimizing Low Dimensional Carbon-Based Nanomaterials For Seawater Desalination: Investigating the Viability of Graphene-Oxide TiO_2-modified Activated Carbon Composite Electrodes for Water Demineralization

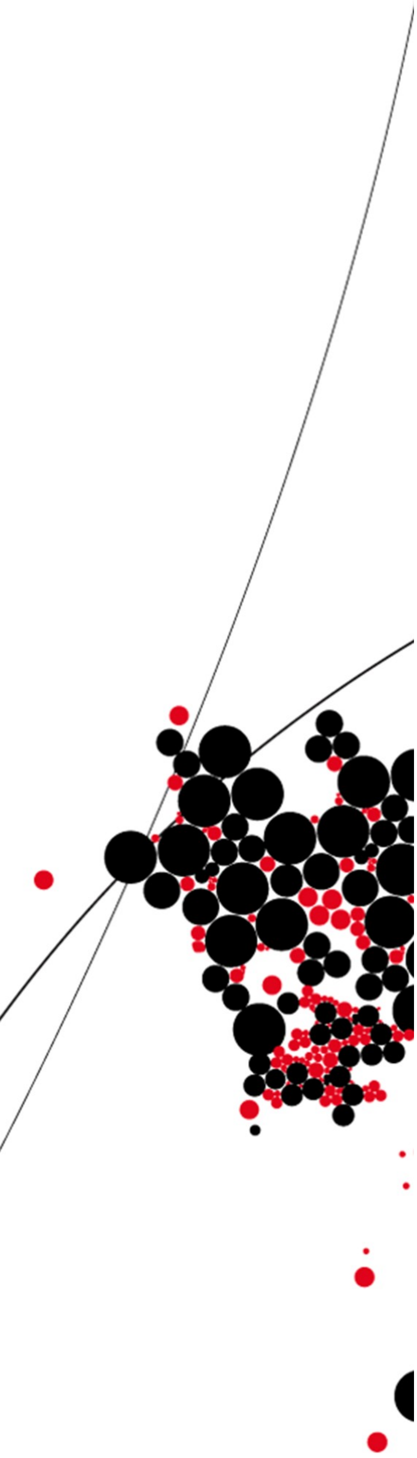

Florian T. H. Kleinhoven
B.Sc. Thesis
May 2019

Supervisors:
prof. Hui Ying Yang
prof. dr. ir. N.E. Benes
prof. dr. ir. R. G. H. Lammertink

Preface

As part of completing my undergraduate education in general engineering with a minor in Bioengineering of the course of Technology and Liberal Arts and Sciences at the University College Twente of the University of Twente in Enschede, The Netherlands, after completing various terms abroad in Brazil, the United States of America and Singapore, I wanted to focus on bringing into practice all of the material science I had learned in the coursework at these various institutions in a project of Civil and Environmental Engineering in a country where water was a particularly precious resource. Although in Singapore water is available in abundance due to the large number of different water recycling facilities and freshwater treatment options, the quality of the water is challenged by changing environmental conditions and the increasing construction of industry in Malaysia and abroad. To ensure the maintenance of healthy water sanitation conditions in Singapore, I wanted to contribute to research and development done in materials engineering in the field. To enhance impact of my project, partnering with the Public Utilities Board (PUB) in Singapore was a logical option. I would like to thank Professor Hui Ying Yang of the Singapore University of Technology and Design (SUTD) for her continued support from reading drafts, to preparing presentations, to connecting me with potential partnering companies. I would like to thank Mien Ling Chong for her support from PUB's side and her continued feedback on the progress of the project. I would like to thank Ding Meng of SUTD for her continued assistance during experiments and in reviewing academic material for the background of the research project. I would like to thank Professor Rob Lammertink and Professor Nieck Benes of the University of Twente for reviewing my final project deliverables.

Summary

Water availability in Southeast Asia has been challenged by a variety of climate change-induced chemical alterations of rainwater. Potable water is increasingly difficult to produce in sufficient quantities to service the world population. Developing as well as developed countries increasingly need to depend on water desalination for their main source of freshwater. According to various studies, the percentage of desalination in the current market will only increase over the next couple of decades. Due to certain chemicals used in industrial processes around the globe, water has been contaminated with a plethora of charged compounds that must be removed to once more create potable water. The presence of these charged compounds forms a special challenge in water sanitation. Especially the presence of valent ions in water, more commonly referred to as water hardness or mineralization, must be addressed in the near future. Due to the demineralization processes involved in water demineralization, often targeting the electrical charge difference of coions in solution, the ability to remove individual cations and anions is severely limited. In the case of Singapore, a well-developed country in the region of Southeast Asia, the water hardness is quantified by $CaCO_3$ and remains at around 80-120 mg L^{-1} after desalination. Optimally, the concentration would be lower than 60 mg L^{-1}. Similarly, Singapore's Public Utilities Board is working hard to reduce the boron concentration to less than .5 ppm in freshly desalinated water. Technologies currently applied in this context include mechanical filtration and reverse osmosis. However, these technologies have as a disadvantage their high energy consumption due to the requirement for artificial pressure generation. Membrane-based capacitive deionization forms a competitive solution to reduce water mineralization levels because of its capacity to electrosorb cations such as Ca^{2+} and B^+ at a large scale. Using an experimental setup with mechanical pressure and a recycling solution of 1 M NaCl broth, this study showed the viability of using TiO_2-coated activated carbon filler in a reduced graphene-oxide matrix for water demineralization at low energy consumption. This study assesses the viability of TiO_2@AC:rGO composite electrodes for MCDI-based demineralization and concluded in a design based on angled coils guiding water by natural pressure generation from gravity for water flux optimization. The prototype design promises functional demineralization capacity using minimal energy from external sources.

Contents

List of acronyms

AC	Activated carbon.
ADC	Affordable Desalination Collaboration.
CDI	Capacitive deionization.
GO	Graphene-oxide.
MCDI	Membrane-based capacitive deionization.
MF	Microfiltration.
NF	Nanofiltration.
ppm	Parts per million.
PUB	Public Utilities Board.
TiO_2	Titanium dioxide.
rGO	Reduced graphene-oxide.
RO	Reverse osmosis.

List of figures

Chapter 1

Introduction

Seawater desalination is the main source of potable water around the world. The report by McGranahan (2002) already suggested water scarcity in Southeast Asia would have increased massively by 2025, requiring further expansion of water desalination plants (McGranahan, 2002; Royan, 2016). Humanity’s modern lifestyle has affected both the availability and viability of water supplies. Fresh water supplies form a major requirement for life and survival but have become an increasingly scarce commodity across the globe. Potable water can no longer be retrieved just from wells and natural water bodies to suffice the needs of a 7 billion strong global population.

Due to certain chemicals used in industry, water has been contaminated with a plethora of charged compounds that now need to be removed from potable water. In countries where water sanitation facilities are insufficiently in operation, this is particularly challenging. Products such as fertilizers used in agriculture, chemicals used in industrial processes, etc. have created an excess of ionic particles that are difficult to remove from water. The presence of positively charged ions in particular has formed a challenge, particularly in countries with insufficient water sanitation facilities are in operation.

Elevated ion concentration is more commonly referred to as water hardness. Developing regions in South and Southeast Asia in particular often rely on primitive desalination technology for their main water source. Additional lacking water sanitation facilities allow persistent water hardness to affect developing regions of the world. Although concrete, quantifiable data is difficult to obtain given the large geographical dispersion of this issue, previous catastrophic events have led to believe the introduction of unnatural elements into the biosphere is typically detrimental. For instance, the lasting presence of hard ions in potable water may have lasting effects on human and environmental health, affecting the natural biosphere as well as causing cardiovascular disease, pulmonary lung disease and being correlated to growth retardation and reproductive failure (World Health Organization, 2011).

Major water desalination technologies rely on membrane technology responding to particle size (Frost & Sullivan, 1975). Solutions such as reverse osmosis and nanofiltration are pressure-driven, largely mechanical in their functioning and hence prone to fouling. Electrochemical methods, precipitation and ion-exchange require significant amounts of energy and complicated architectures to accommodate them. Moreover, chemical techniques often require extensive post-treatment to minimize the environmental impact.

Membrane-based desalination suffers extensively from fouling and only permits limited pressurized water flux (Malaeb & Ayoub, 2011) Recent innovations have focused on exploring electrochemical reducing energy consumption of desalination, whilst permitting higher permeation flux to upscale technologies (Li & Yeo, 2011). Carbon-based capacitive deionization can be modified for different architectures relatively easily and cheaply, and consumes less energy than traditional electrochemical methods. These technologies currently range anywhere from approximately 1.0 kWh m^{-3} to more than 7.6 kWh m^{-3} of potable water. Additionally, carbon-based materials are known for being easily regenerated at low costs. Especially in developing countries where remnant ions in water are a challenge and the overall cost of a solution is a limiting factor. For future expansion of the technology, choosing one that will optimize functionality and cost is preferable.

Membrane-based capacitive deionization, a carbon-electrode based technology for water demineralization is particularly attractive for application in low-resource regions because of its potential using only electrical energy for the electrodes. Furthermore, because of the nature of the membrane application in MCDI, fouling is prevented by the use of electrochemical washing, rendering the technology more durable than more traditional alternatives.

This paper explores the use of activated carbon (AC) electrodes in graphene-oxide matrix structures to optimize 2D architecture integrity while maintaining high conductivity for membrane-based capacitive deionization (MCDI). In the broader context of water desalination in Southeast Asia, the study investigates the feasibility of introducing graphene-oxide TiO_2-modified activated carbon composite capacitive deionization as a viable second-line post-desalination treatment of water. This study also investigates the theoretical benchmarking qualities of graphene-oxide TiO_2-modified activated carbon composite activated carbon for water demineralization because of their ability to remove positively charged boron and calcium ions. The chief factors includes in this study are demineralization capacity, energy consumption and electrode half-life. The study hypothesizes that the demineralization qualities of graphene-oxide TiO_2-modified activated carbon composite electrode materials combined with the lower energy consumption rates will outweigh the efficiency benefits of traditional technologies.

Chapter 2

Background

Traditional demineralization techniques use mechanical pressure-based systems such as multiple cycles of micro- and nanofiltration (NF) and reverse osmosis (RO) (Izadpanah & Javidnia, 2012; Eriksson, 1998; Ramen, et al., 1994; Shon, et al., 2013; Efraty, et al., 2011; Song, et al., 2012). These types of systems help to provide a high flux at lower operation pressures while maintaining optimal salt rejection rates (Izadpanah & Javidnia, 2012; Eriksson, 1998; Ramen, et al., 1994; Shon, et al., 2013; Efraty, et al., 2011; Song, et al., 2012). Such purely membrane-based technologies are often adversely affected by chemical interactions between suspended solutes in the mixture and the membrane material. To address the issue of chemical solute interaction, a more sophisticated understanding of the chemical interaction is required but remains to this day insufficient to design more cost-effective solutions.

Alternative technologies such as thermal distillation, composite materials, and hybrid technologies often suffer from the need of artificial, external pressurization and lower pressure-recovery rates than membrane technologies (Stover & Efraty, 2011; Song, et al., 2012; Stover, 2013; Kabeel, et al., 2013; Jeong, et al., 2007; Subramani & Jacangelo, 2015; Rovel, et al., 2003). Technologies requiring external pressurization are hence subject to significantly larger energy consumption rates than the aforementioned membrane-based technologies. For comparison, while most membrane filtration plants operate at an average pressure of 7 to 30 bars (Shon, et al., 2013). In the context of Singapore, the energy consumption would balance at an average of 3.5 kWh m^{-3}, according to interviews conducted at the Public Utilities Board. Hybrid plants often consume up to 7.6 kWh m^{-3} and can only maintain fluxes of approximately 26.1 to 43.7 L m^{-2} h^{-1} (Song, et al., 2012; Stover, 2013; Hemmatifar, et al., 2016). Ideally, the net energy consumption would be lower than 1.0 kWh m^{-3} after energy recovery.

The challenge of water hardness (mineralization) — a measure for the number positively charged ions (cations) suspended in solution — in particular remains challenging in the context of Southeast Asia. Mineralization is quantified by the concentration of $CaCO_3$ in solution (Gabelich, et al., 2002). However, the effects of Ca^{2+} counterparts such as Mg^{2+}, B^+ and Fe^{3+} might entail severe consequences for human and environmental health. (Gabelich, et al., 2002). Mineralization levels in natural water bodies have never reached the desired level of 60 ppm but remain around 80-120 ppm (World Health Organization, 2011) B^+ is of particular interest because of its severe effects on essential metabolic features, including calcium-utilization for brain function, psychomotor responses (Nable, et al., 1997; Nielsen, 1997).

This paper proposes to use a composite material in an electrochemical method called membrane capacitive deionization (MCDI). In an MCDI plant, saline solutions are pushed through unrestricted capacitor modules constructed of high-surface area electrode, guided by often polymeric ion-exchange membranes (Subramani & Jacangelo, 2015). Compared to NF and RO, MCDI was able to operate at as low an energy consumption as 1.65 kWh m^{-3} according to the Public Utilities Board. MCDI is a particularly attractive option to affect reduction of water mineralization because of its ability to electrosorb cations upon polarization of the electrodes (Welgemoed, 2005; Subramani & Jacangelo, 2015). Similarly, because of a lack of fouling, electrochemical methods such as MCDI remain much more reliable than NF and RO (Lee & Lee, 2000; Park, et al., 2016). Unfortunately, however, due to the complicated architecture required to run MCDI at a large scale, this technology has been considered to a limited extent (Galama, et al., 2014; Dey, et al., 2007; Berakat, 2011; Entezari & Tamasbi, 2009).

Based on an easily scalable architecture of stackable, cylindrical layers, this paper proposes to use MCDI for demineralization purposes in contexts of the developing world in particular. This paper experimented with MCDI electrodes fabricated from TiO_2-coated AC (TiO_2@AC) in a reduced graphene-oxide (rGO) matrix to optimize 2D nanostructure for stability whilst maintaining the high electrical conductivity of AC electrodes (Kim & Choi, 2010). AC electrodes pose an attractive option because of its high potential degree of porosity, specific surface area and absorption capacity (Rettier, et al., 2012). This study aims to study the demineralization performance of TiO_2@AC:rGO composite electrodes for applications in the context of developing countries.

2.1 Global Desalination Market

In 2010, the global water market amounted to US$ 425 billion with key activities in construction, technological engineering and design (Royan, 2012). By 2016, the total global water market had grown to a US$ 625 billion business (Royan, 2016). According to Frost and Sullivan, a British engineering consultancy, in 2015, 36% of the total business is in the development of new technologies, of which a respective 54% is wastewater treatment and another 32% is water treatment for the creation of potable water. Based on data from 2015, Frost and Sullivan forecast that a small fraction on the crossover between water and wastewater treatment will provide a sizable market share over the course of the next decade. In total, 11% of water treatment technologies are wastewater treatment oriented (Royan, 2012; Royan, 2016). Similarly, the wastewater treatment technologies have seen a steady increase in capacity in Asia Pacific over the course of the years from 2015 till 2019 and are projected to continue increasing until 2022 (Royan, 2016).

Figure 2.1.1: Global market share of water treatment (adapted from Royan, 2016).

Freshwater is a requirement for life and survival and yet has become an increasingly scarce commodity across the globe. From droughts in California requiring the external import of potable water to pollution in Malaysia disabling the population’s water consumption to the seasonality in the tropics rendering consistent water collection from catchments virtually impossible, all life requires freshwater. Potable tap water has become a commodity the West has grown used to and expects every day. Potable, or at the very least tolerable water, however, has become something of a luxury item. Countless nations across the world cannot guarantee that the water they drink will sustain them for the years to come. Water sourced near areas commonly used for agriculture or industry can often be contaminated with cadmium, led or mercury leading to a range of debilitating diseases (United Nations, 2009). Providing more affordable and healthier solutions to generating freshwater should hence be a priority to the world.

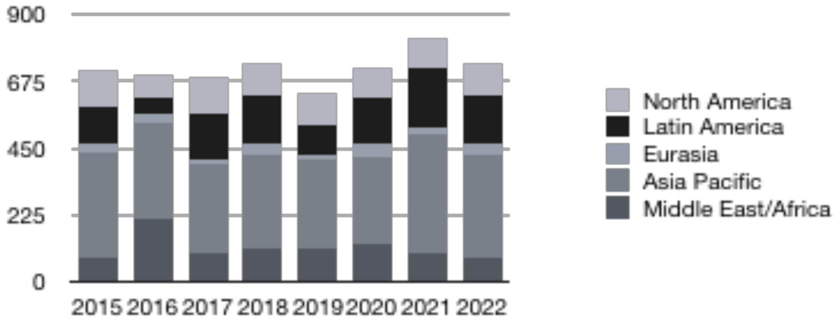

Figure 2.1.2: Global market share of water production 2016–2023 (adapted from Global Water Intelligence, 2018).

Frost and Sullivan provided an overview of the uses of particular technologies in water desalination around the world. Since 1975, there has been a steady increase in the number of desalination plants being built in the world. As the report by McGranahan (2002) suggests, the water scarcity in Southeast Asia will increase massively by 2025, rendering the construction of sufficient water sanitation plants evermore paramount. Currently, the overall global desalination capacity is already at around 18 billion liters per day (Royan, 2016). Unfortunately, however, this is not enough to provide the capacity needed to sustain Southeast Asia's growing population. Due to elevated living standards, growing populations tend to consume increasingly excessive water at incrementally larger scales. Southeast Asia in the future will need increasing capacity to generate large quantities of potable seawater for a growing population and increasing agriculture demands (Royan, 2016).

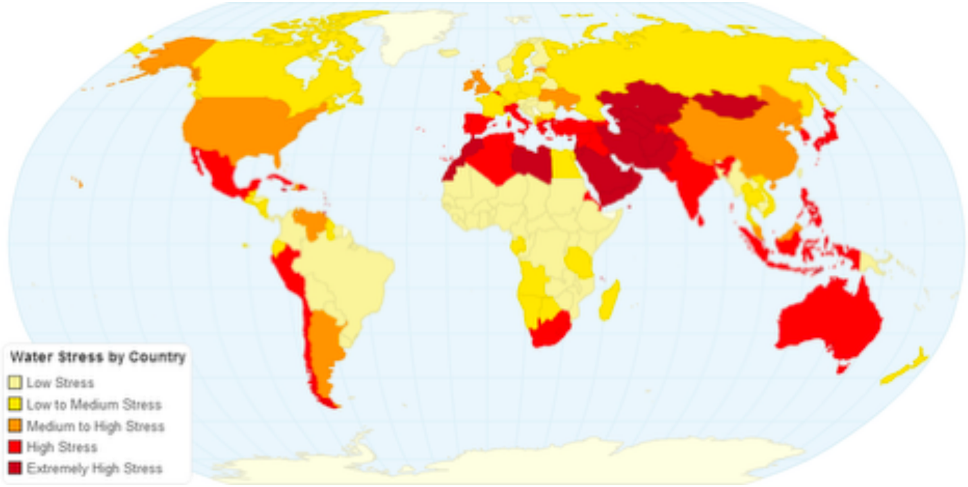

Figure 2.1.3: Global water stress and scarcity by 2025 (adapted from McGranahan, 2002).

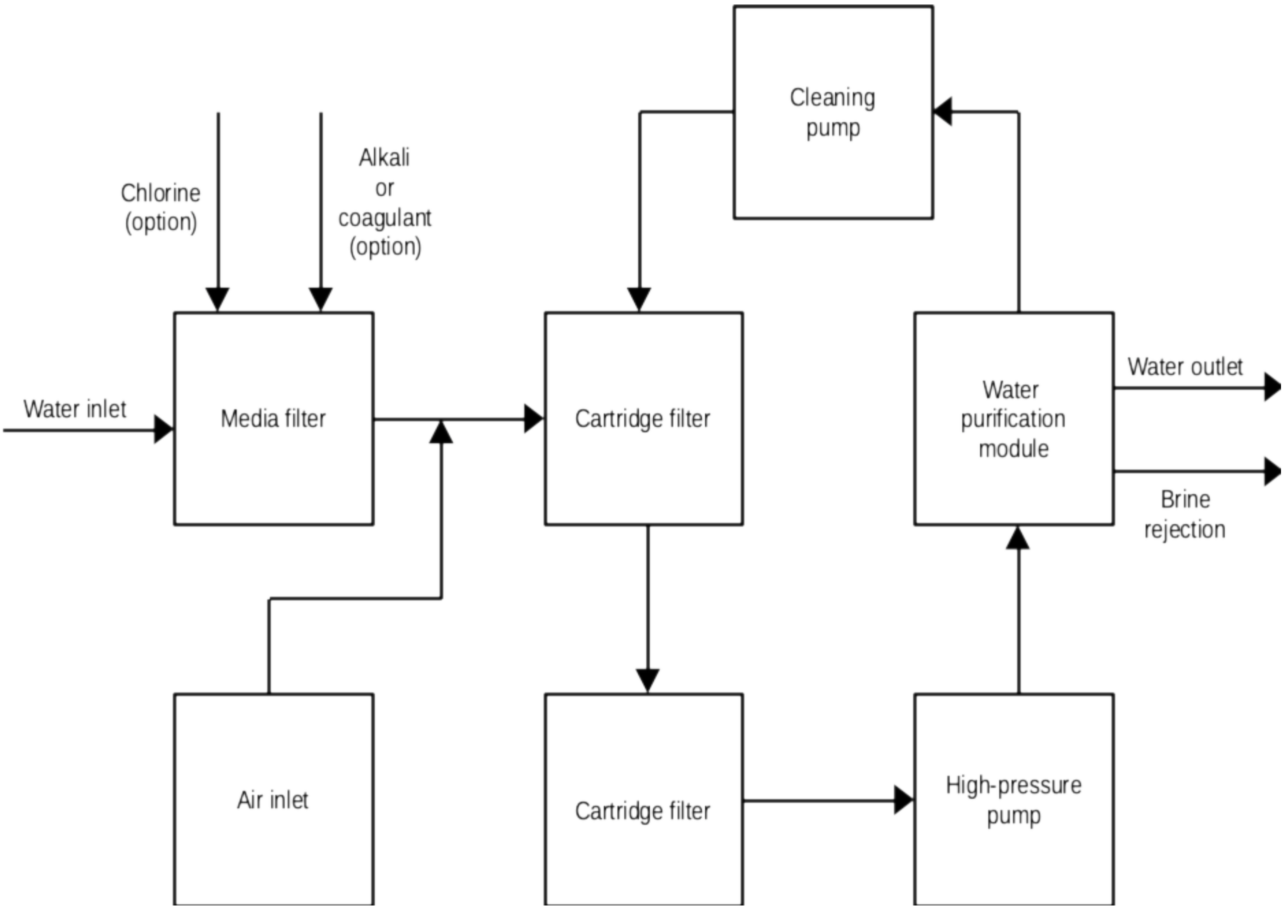

Figure 2.1.4: Generic overview of water desalination process (from Li & Yeo, 2011).

The most obvious solution to generating large quantities of potable freshwater in coastal areas is desalinating seawater. Over the course of the past few decades, the majority of research in desalination technology has been focused on membrane-based technologies. This is in the first place due to their supposed ability to operate at relatively low chamber pressures, require less energy and are optimizable for high-flux systems. More recent innovations, however, have been focusing on reducing the energy consumption of the desalination process (Peñate & García-Rodriguez, 2012). Modern research also focuses on looking for technologies, which would permit higher permeation flux in the system (Malaeb & Ayoub, 2011). Furthermore, research since the beginning of the decade has been concentrating on minimizing the negative effects of fouling that tend to occur when systems are upscaled to allow (Malaeb & Ayoub, 2011). However, since this paper will focus on electrochemical methods of desalination, reducing the fouling effect of bioreactors is beyond the scope of this research.

2.2 Water Hardness

Due to the chemical processes involved in water desalination, the hardness of desalinated water remains relatively uncontrolled throughout the development of desalination techniques. According to PUB, the current procedure at the NEWater facilities requires the water to be alkaline at pH 10–10.5 to be able to be desalinated (Chong Mien Ling, personal communication, February 22, 2019). Due to the nature of alkaline conditions, the charge of the water changes in such a way as for the difference to render cations unrecognizable. For instance, in Singapore, the majority of desalination plants are designed to deliver water with a hardness of approximately 80-120 mg L^{-1} $CaCO_3$, whereas ideally the concentration should be below 60 mg L^{-1} (World Health Organization, 2011). Water hardness is a measure of the amount of calcium and magnesium salts in water. The more calcium and magnesium in water, the harder the water. Water hardness is usually expressed in milligrams per liter (mg L^{-1}) of dissolved calcium and magnesium carbonate. In developing countries in the same region, facilities management and citizens often fail to gain access to the equipment necessary to measure the hardness of the water (Sengupta, 2013). Elevated levels of calcium, magnesium, and barium levels in potable water might cause health challenges such as increased prevalence of cardiovascular disease, growth retardation in infants and reproductive failure in adults (World Health Organization, 2011). Increased hardness of water could pose challenges to the environment due to elevated levels of nitrogenous species (Sengupta, 2013). The presence of these ions also correlates to increased levels of soil and water pollution caused by the use of fertilizers in agriculture. This research project investigates the efficacy of removing singular cations from aggregate potable water in addition to reducing the total amount of energy needed for successful demineralization. Especially in regions where energy is a scarce resource, such as many countries in Southeast Asia, addressing this challenge is a major concern.

As per Gabelich, et al. (2002), the most prevalent cations present in desalinated water are Ca^{2+}, Mg^{2+}, B^+ and Fe^{3+}. Although research into sea salt removal and single-ion salt removal has been ongoing for various decades, more complex multi-ion salt experiments have rarely been attempted. This study will focus on the use of capacitive deionization using increased negative surface charge on a pair of carbon-based electrodes. The main advantage is that the ions will be electrostatically desorbed into a waste stream. Earlier work has already been performed to examine the competitive removal of various hardness-related ions, but no quantitative study has yet been provided to show the desorption performance of particles such as Na^+, Mg^{2+}, K^+, Rb^+, Cl^-, Br^-, NO_3^- and SO_4^{2-}.

Boron in particular is distributed in a wide variety of elements in nature and appears in the form of boric acid or borate salt (García-Soto & Camacho, 2005; Fujita, et al., 2005). Although boron is essential to the maintenance of life, boron can be harmful to delicate balances of life, including metabolic features such as calcium-utilization, brain function, psychomotor responses, and estrogen ingestion in the human body (Nable, et al., 1997; Nielsen, 1997). According to the guideline standards set by the World Health Organization (WHO) for drinking water, the acceptable boron concentration must be ≤ .5 ppm (mg L) for default quality potable water (Köse, et al., 2011).

However, removing boron from water is difficult, especially since the pH has to be adjusted to levels of 10.5 ± .5, which renders the technique prohibitively expensive and impractical (Chong Mien Ling, personal communication, February 22, 2019). The most feasible experimental method for boron removal is chemical activation of the nano filtration technology, consisting of impregnating the solution with some metal-oxide and removing the bonded metal-oxide using some filtration technique (Nakagawa, et al., 2007).

2.3 Competitive Landscape

The majority of experimental technologies for water purification work based on a combination of charge and size-based selectivity. The objective is to optimize the efficacy of both actions in water demineralization, to attain the purest and healthiest, potable water. The ensuing paragraphs will summarize the main technologies currently used in water desalination in order to be able to compare and contrast their optimization and energy usage under different conditions for different manufacturers.

According to Dundorf, et al. (2009) and Puyol (2009), the average energy consumption of RO plants can be as low as 2.0 kWh m^{-3} of water produced. Similarly, the average of RO energy consumption has been found to be no lower than between 2.2 and 2.5 kWh m^{-3} of water produced (Ludwig, 2009; Stover, 2009). The most obvious approach to reducing the energy in desalination plants is to increase energy recovery using other third-hand technologies. For instance, energyry devices based on isobaric chambers and positive displacement pumps integrated in reverse osmosis (RO) facilities have yielded over 90% in energy retrieval (Peñate & García-Rodriguez, 2012). The ability to recycle energy significantly reduces the strain destination plants place on the energy net around them as well as the economic burden of freshwater. Furthermore, Affordable Desalination Collaboration (ADC), a Californian non-profit desalination research institute has shown that the majority of technologies can operate under similar energy consumptions based on optimization for different circumstances (Puyol, 2009).

Nanofiltration. Nanofiltration (NF) membranes are known for their ability to provide a high water flux at low operating pressure and maintaining a high salt rejection rate, rendering them highly efficient at mineral removal (Eriksson, 1998; Ramen, et al., 1994). NF membranes would also pose a solution in demineralizing water for hardness reduction purposes (Izadpanah & Javidnia, 2012). Attaining water vapor by operating nanofiltration processes at higher temperatures and chamber pressures has been shown to deliver the purest permeate (Shon, et al., 2013). Nanofiltration membranes ideally retain co-ions of up to 1–5 nm pore size and operate at pressures between 7 and 30 bars. However, NF membranes suffer from fouling — the process whereby a solution or a particle is deposited on a membrane surface or in membrane pores in a processes such as in a membrane bioreactor, reverse osmosis, forward osmosis, etc. In water desalination, NF membrane fouling might occur especially due to inorganic particle precipitation during scaling, colloidal residue and organic absorption (Shon, et al., 2013).

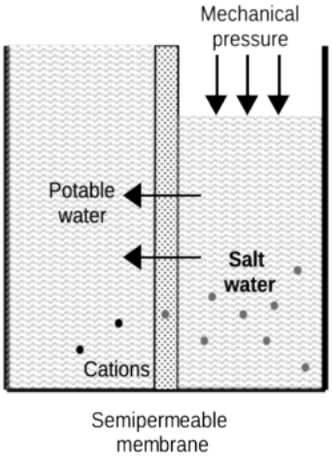

Figure 2.3.1: Nanofiltration process (adapted from Li & Yeo, 2011).

Membrane-based reverse osmosis. Reverse osmosis (RO) is a water purification technology that uses a semipermeable membrane to remove ions, molecules and larger particles from drinking water. In RO, a solvent passes through a porous membrane in the direction opposite to that for natural osmosis when subjected to a hydrostatic pressure greater than the osmotic pressure. The reverse osmosis process is exemplified in Figure 6 (Li & Yeo, 2011). Optimal RO processes combine raw feed water and circulating concentrates, which lower the feed pressure required for desalination and demineralization (Efraty, et al., 2011; Song, et al., 2012). RO processes can operate at pressures as low as 40 bar, compared to the normal high of 70 bar (Stover & Efraty, 2011).

Various experiments have been conducted in which the energy consumption was measured to be approximately 0.64 and 0.76 (and as high as 1.0) kWh m^{-3} at brackish water fluxes between 26.1 and 43.7 L m^{-2} h^{-1} (Song, et al., 2012; Stover, 2013). At an average flux of 20.1–28.4 L m^{-2} h^{-1} the maximum recovery in one experiment was 94% (Stover, 2013).

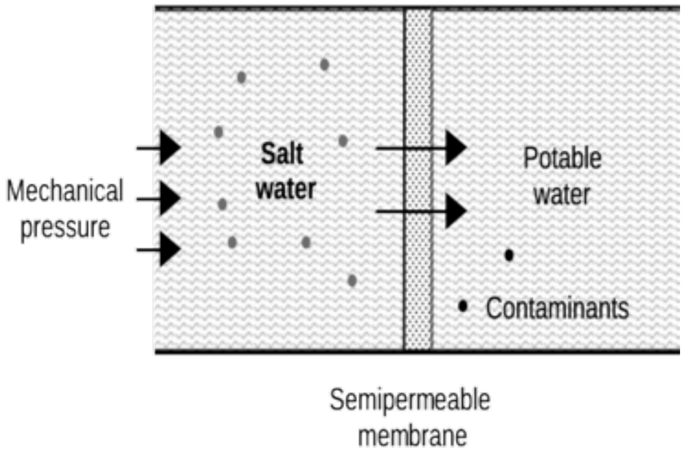

Figure 2.3.2: Reverse osmosis process (adapted from Li & Yeo, 2011).

Thermal distillation. Membrane distillation is a thermally driven fluid separation process where a micro-porous hydrophobic membrane separates two aqueous solutions at different temperatures. The hydrophobicity of the membrane prevents mass transfer of the liquid, whereby a gas-liquid interface is created. Due to the phase change, the hydrophobic membrane displays a barrier for the liquid phase, allowing the vapor phase to pass through the membrane's pores. The most obvious example of thermal distillation is humidification-dehumidification (HDH), a distillation process functioning on air’s ability to carry water vapor at higher temperatures than its boiling point (Kabeel, et al., 2013). The system consists of a humidifier, a dehumidifier and a heater for the carrier gas and the feed water stream (Narayan, et al., 2009; Narayan, et al., 2010). The air is saturated with heat before further heating and humidifying the system. Tests run on Celgard Ligui-Cel® Extra-Flow 2.5X8 contactors with X-30 and X-40 hydrophobic fiber membranes 10 mg L^{-1} seawater at low heat showed little economic competitiveness (Evans & Miller, 2002). This configuration resulted in a lower energy consumption of approximately 120 kWh m^{-3} (Holst, 2007).

Adsorption desalination. Adsorption desalination employs water vaporization followed by vapor adsorption into highly porous silica gel (Ghaffour, et al., 2014). The water is vaporized at low temperatures using waste heat from nearby industry (Ng, et al., 2013).

The water generated using this method is nearly pure at a specific energy consumption of less than <1.5 kWh m^{-3} of clean water (Subramani & Jacangelo, 2015). However, a range of specific conditions in environmental infrastructure and energy provision is required in order to feasibly implement this technology for water desalination. Similarly, pervaportation is based on the separation of aqueous salts in pseudo-liquid mixture containing free water molecules and bulkier hydrated ions upon dissociation from the salt water (Kuznetsov, et al., 2007). Using polyvinyl alcohol (PVA) based membranes or polyetheramide-based polymer film of 40 μm thickness, a total retention of 99% for all ions was achieved, which was significantly higher than reverse osmosis (Zwijnenberg, et al., 2005). At an operational temperature of 50 °C the maximum water flux was 26.4 L m^{-2} h^{-1} (Hamouda, et al., 2011).

Hybrid solutions. The Saline Water Conversion Corporation (SWCC) deployed a hybrid plant composed of reverse osmosis (RO) and multiple-stage flash desalination (Hamed, 2005). By combining these two technologies, the plants can respond to smaller and larger water demand with its projected operational capacity totaling at about 725.4 mgd (2.74 Mm^3 d^{-1}), of which only 10% is yielded through RO (Al-Mutaz, 1996). The MSF and RO plants also share the intake and outfall facilities, combining the products of two processes into one.

Sarkar and Sengupta (2008, 2009) proposed a further refinement of the hybrid technology by integrating NF, RO and ion-exchange technologies. These combined technologies are considered useful to remove boron and other cations from permeates of RO desalinated water because of boron's particularly harmful effects to human health (Sengupta, 2013). In their experiment, polymeric ion exchange resins were used to convert the monovalent cations to divalent cations to facilitate more effective removal using NF (Sakar & Sengupta, 2008). NF then achieved a 98% rejection rate of various saline solutions at 0.9 kWh m^{-3} water produced (Sakar & Sengupta, 2009). This experiment, however, requires two desalination phases with an ion exchange filter, equating to higher energy levels in total.

According to Dundorf, et al. (2009) and Puyol (2009), the average energy consumption of RO plants can be as low as 2.0 kWh m^{-3} of water produced. Similarly, the average of RO energy consumption has been found to be no lower than between 2.2 and 2.5 kWh m^{-3} of water produced (Ludwig, 2009; Stover, 2009). The most obvious approach to reducing the energy in desalination plants is to increase energy recovery using other third-hand technologies. For instance, energyry devices based on isobaric chambers and positive displacement pumps integrated in reverse osmosis (RO) facilities have yielded over 90% in energy recovery (Peñate & García-Rodriguez, 2012). The ability to recycle energy significantly reduces the strain destination plants place on the energy net around them as well as the economic burden of freshwater.

Furthermore, Affordable Desalination Collaboration (ADC), a Californian non-profit desalination research institute has shown that the majority of technologies can operate under similar energy consumptions based on optimization for different circumstances (Puyol, 2009).

Sarkar and Sengupta (2008, 2009) proposed a further refinement of the hybrid technology by integrating NF, RO and ion-exchange technologies. These combined technologies are considered useful to remove boron and other cations from permeates of RO desalinated water because of boron's particularly harmful effects to human health (Sengupta, 2013). In their experiment, polymeric ion exchange resins were used to convert the monovalent cations to divalent cations to facilitate more effective removal using NF (Sakar & Sengupta, 2008). NF then achieved a 98% rejection rate of various saline solutions at 0.9 kWh per meter cubed water produced (Sakar & Sengupta, 2009).

Other promising technologies, such as carbon nanotube membranes, based solely on carbonic molecular properties seem promising but remain experimental for the time being. Although nanotubes appeared to exhibit water mass transport larger than 2 to 5 times that of normal reverse osmosis processes, the range in diameter for ions is limited between 6–11 Å (Holt, et al., 2006; Ahadian & Kawazoe, 2009). Similar to carbon nanotubes, boron nitride nanotubes exhibited far superior water flow rates, but with limited pore sizes of up to 4.14 Å for average cation selectivity and 5.52 Å for average anion selectivity (Hilder, et al., 2009). Even though nanotubes have been shown to be able to operate sufficiently under reduced hydraulic driving pressures and consume less energy, the thermodynamic strain imposed on osmotic pressure-driven gradients renders the process usable (Song, et al., 2003).

2.4 Capacitive Deionization

Nanofiltration and reverse osmosis are both durable solutions to water demineralization. However, these technologies require intermittent cleaning using citric acid to counteract fouling and must be replaced every 1000 cycles. Capacitive deionization (CDI) is the process in which saline solutions flow through unrestricted capacitor modules constructed of high-surface area electrodes (Welgemoed, 2005). CDI is an alternative technology to RO and NF and can operate at much smaller scales, produce significantly smaller hardness levels and work with large surface areas (400-1100 m^2 g^{-1}) and low electrical resistivity (< 40 mΩ cm^{-1}) (Welgemoed, 2005). CDI is particularly attractive for reducing water hardness in low-resource regions because of its ability to electrosorb cations and anions upon polarization of electrodes (Subramani & Jacangelo, 2015). Similarly, unlike common electrochemical methods, CDI does not require the use of mechanical pressure to operate.

Membrane-based CDI is attractive because it requires significantly less energy than most traditional water demineralization techniques (Oren, et al., 2008; Greenlee, et al., 2009; Malaeb & Ayoub, 2011; Zhao, et al., 2013; Kucera, 2014). Despite the low salt adsorption capacity of CDI, especially at low frequencies and voltages and high salt concentrations, its use in demineralization is not limited since it only has to sustain a high cation selectivity (Lee, et al., 2014; Ding, et al., 2017). The potential for low-energy consumption and partial energy recovery in CDI upon demineralization makes it an ideal candidate for demineralization of desalinated water hardness (Długołęcki & van der Wal, 2013; Zhao, et al., 2013).

Efficiency can be further improved using membrane technology (Kim & Choi, 2010). Using membrane technology, the device can be constructed in such a way as to allow the water to flow through the electrodes instead of between them, optimizing the desalination potential at lower energy consumption (Kim & Choi, 2010). In CDI, the electric field is used to draw cations and anions from the solution across the ion-exchange membranes on both sides of the reactor. The electrode surfaces are covered with cation- or anion-selective membranes , which are always wired in series to optimize salt filtration effects for coins (Subramani & Jacangelo, 2015). Water is passed through a space between the opposing electrodes, water flows across the membranes, where cations and anions can accumulate within the porous electrode structure (Voltea, 2012). This combination of electrodiffusion and CDI is called the Voltea process and is the most optimal iteration of CDI desalination, with 99% salt rejection at less than 1.0 kWh m^{-3} for 3000 mg L^{-1} salinity removal (Subramani & Jacangelo, 2015). The total water recovery including cation removal amounted to 90% recovery (Subramani & Jacangelo, 2015). Especially in low-resource and developing regions, energy consumption is a relevant concern to make a technology implementable at the lowest possible cost and impact on the socioeconomic environs.

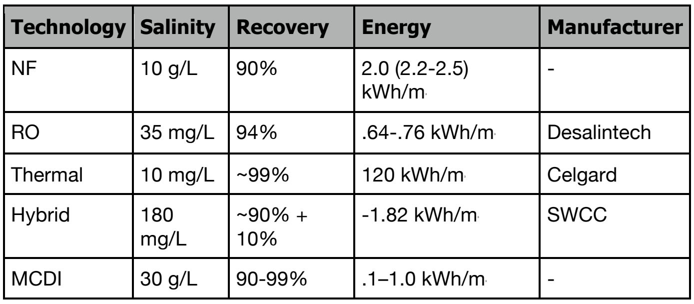

Technology	Salinity	Recovery	Energy	Manufacturer
NF	10 g/L	90%	2.0 (2.2-2.5) kWh/m	-
RO	35 mg/L	94%	.64-.76 kWh/m	Desalintech
Thermal	10 mg/L	~99%	120 kWh/m	Celgard
Hybrid	180 mg/L	~90% + 10%	-1.82 kWh/m	SWCC
MCDI	30 g/L	90-99%	.1–1.0 kWh/m	-

Figure 2.4.1: Quantitative comparison of the performances of desalination technologies (adapted from Welgemoed, 2005; Siemens, 2014; Song, et al., 2012; Stover, et al., 2013).

2.5 Composite Electrode Materials

In this study, the Voltea process was integrated into the electrode fabrication by constructing composite electrodes from TiO_2@AC:rGO. As outlined in the study by Otowa, et al. (1993; 1994; 1997), using the filler-matrix principle in activated carbon based electrode fabrication has the potential to optimize the surface area available in its pores up to 3000 $m^2\ g^{-1}$ for a surface functionality to carbon ratio of approximately 1:4. This observation was further supported by Li, et al. (2012), who emphasized the possibility of creating a filler-matrix structure using the radical oxygen functional groups. In this study, the method by Li, et al. (2012) was used to increase the surface area as a direct result of the surface functionalities present on the activated carbon filler once mashed into the graphene-oxide matrix. Various studies, among which Otowa, et al. (1997), have discovered that the demineralization rate vs. the Brunauer–Emmett–Teller surface area increased proportionally regardless of the remaining surface functionalities due to thermal degradation as a result of repeated hydrothermal reduction of the graphene-oxide. Furthermore, in line with Köse, et al. (2010), the optimal surface area for porous activated carbon electrodes was around 520 ± 280 $m^2\ g^{-1}$, feasibly achievable with the activated-carbon graphene-oxide filler-matrix structure proposed in this paper.

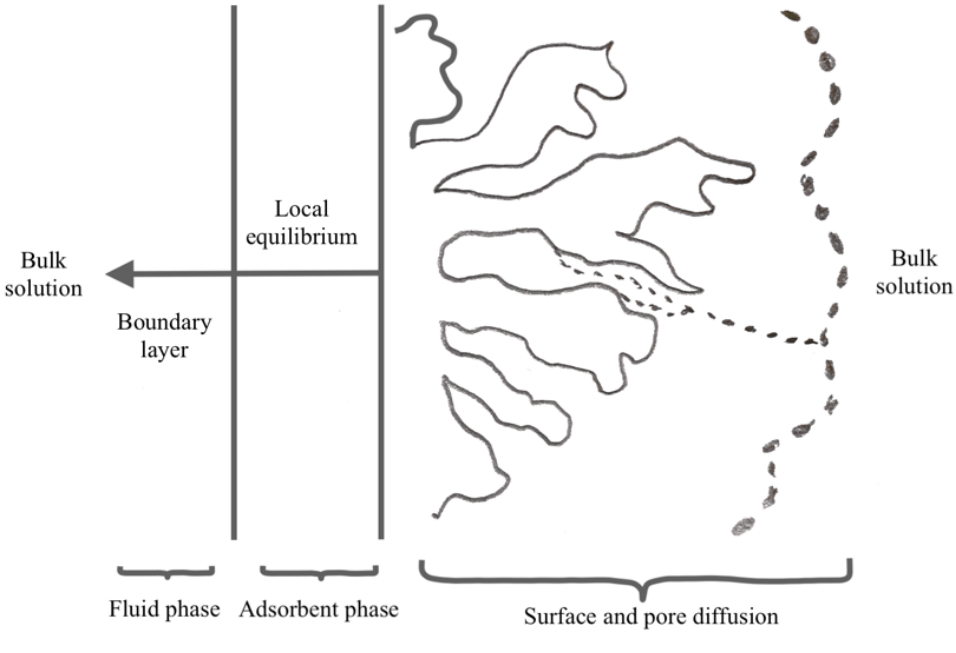

Figure 2.5.1: Mass transfer mechanism in activated carbon-based adsorbents (adapted from Carpenter, et al., 2011; Jarvie, et al., 2005).

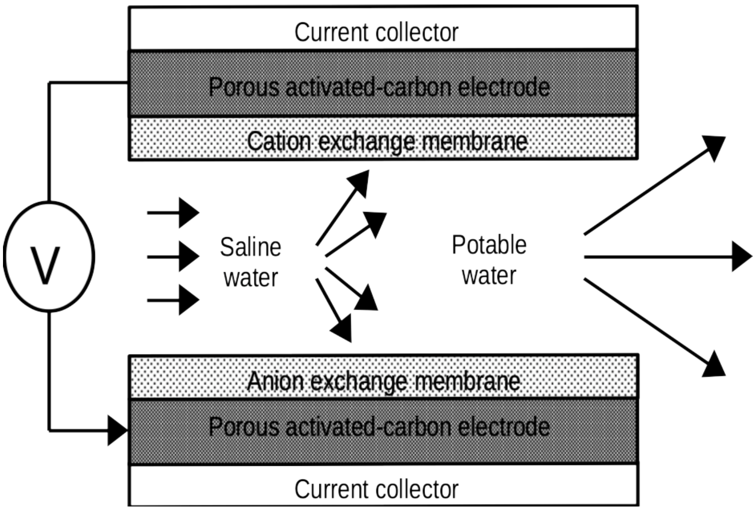

Figure 2.5.2: Membrane Capacitive Deionization (adapted from Gabelich, et al., 2002).

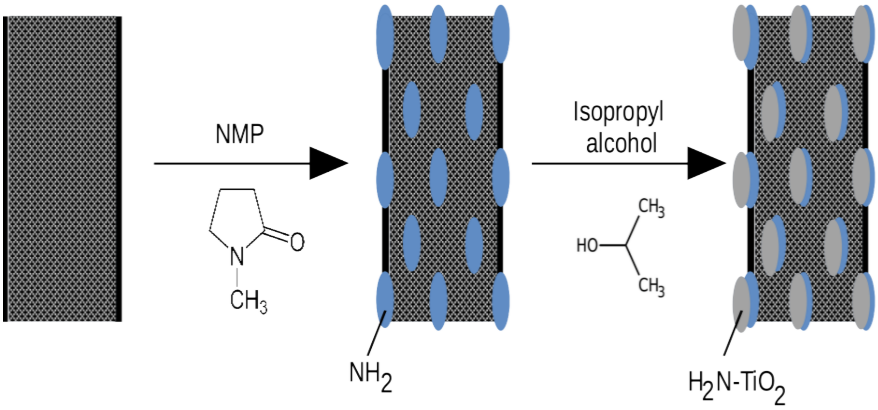

Figure 2.5.3: Schematic overview of the preparation of TiO2-coated activated carbon (adapted from Korhonen, et al., 2012).

In this study, the method by Li, et al. (2012) was used to increase the surface area as a direct result of the surface functionalities present on the activated carbon filler once mashed into the graphene-oxide matrix. Otowa, et al. (1997) discovered that the demineralization rate vs. the Brunauer–Emmett–Teller surface area increased proportionally regardless of the remaining surface functionalities due to thermal degradation as a result of repeated hydrothermal reduction of the graphene-oxide. Furthermore, in line with Köse, et al. (2010), the optimal surface area for porous activated carbon electrodes was around 520 ± 280 m^2 g^{-1}, feasibly achievable with the activated-carbon graphene-oxide filler-matrix structure proposed in this paper.

In this experiment, the findings were based on reduced graphene-oxide composites filled with functionalized AC modified with TiO_2 crystals on its surface structures. According to Li, et al. (2012), a composite material of graphene-oxide and functionalized activated carbon would show great potential in effective demineralization of brackish water as well as maintain cation-selective properties over the course of its usage. More specifically, graphene-oxide was shown to perform as an effective matrix for the TiO_2 AC filler (Li, et al., 2012). Together, these elements exhibited the ability to construct a high-performance superconductor network.

Hydrothermal reduction of graphene-oxide is a combination of ring-opening of epoxy-groups and forming hydroxyl groups on the edges and in the basal planes under thermal treatment (Pei & Cheng, 2012). The reactions conducted under alkaline conditions were also preferred because of the ability to restore π-conjugated domain and remove oxygenated groups such as epoxy, ether, and hydroxyl upon molecular bonding to filler particles (Zheng, et al., 2017).

For the purposes of this experiment, the graphene-oxide TiO_2-coated activated carbon electrodes will be encapsulated by plain copper electrodes guiding both the electrical signal and providing a surface for pressure inside the device. Based on the data resulting from these assessments, the electrodes will be compared to other technologies for which benchmarking was available from previous studies for the purpose of post-desalination demineralization in low-resource countries.

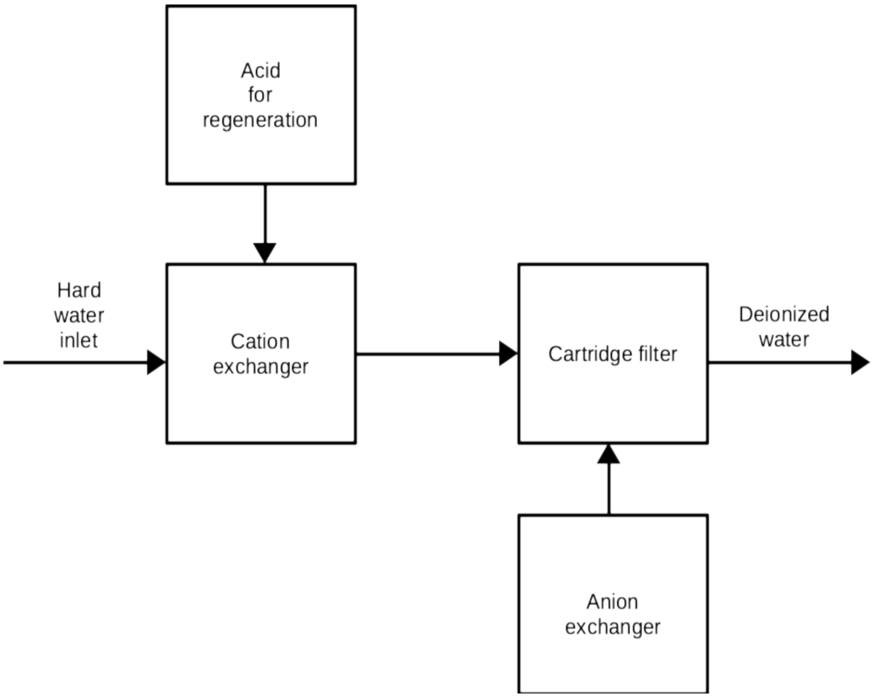

Figure 2.5.4: Generic ion-exchange-based water demineralization process (from Tavani, et al., 1971).

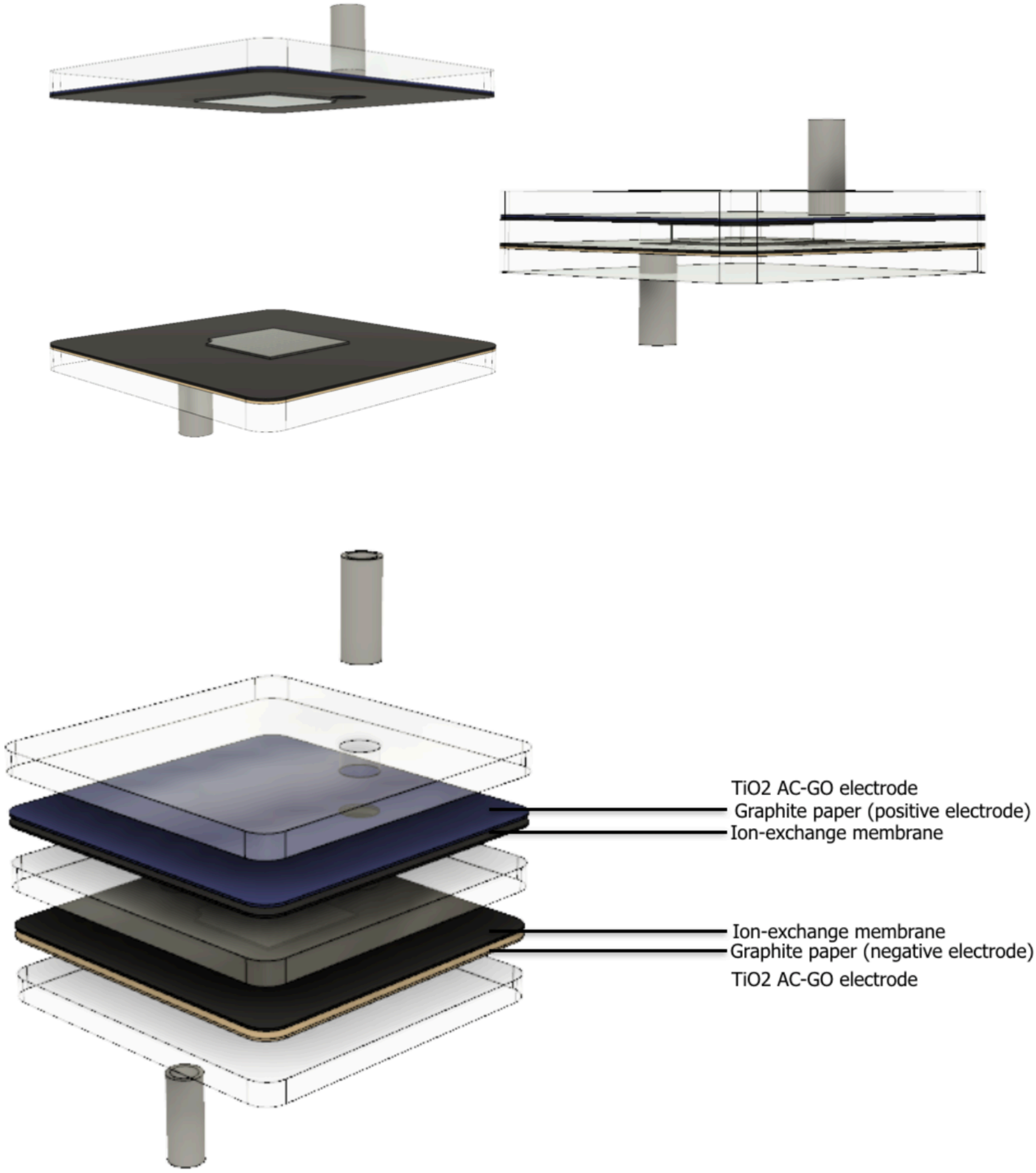

Figure 2.5.5: Schematic overview of copper-based TiO_2-coated AC-GO composite electrodes**.**

2.6 Upscaling Electrode Fabrication

Resin-enhanced rolling activated carbon electrode for efficient capacitive deionization might be utilized to construct a large-scale demineralization bioreactor (Li, et al., 2017). MCDI has thus far been established as a viable technology for post-desalination treatment demineralization, but electrode material remain a major obstacle when upscaling to plant-sized materials (Li, et al., 2017). As described in the experiment by Li, et al. (2017), directly incorporating ion-exchange resins into activated carbon electrodes via the previously described rolling press method might significantly improve the demineralization performance in larger chambers. According to preliminary examinations, the improvement was from anywhere between 41 and 47% up to 121 and 131% for a solution of 0.5 and 2.0 g/L 12.7 and 18.3 mg NaCl (Li, et al., 2017).

Instead of using the method for three-dimensional graphene-oxide composites as structured activated carbons for capacitive desalination described by Leong, et al. (2019), hybrid resin-resin-activated carbon electrodes were fabricated by directly immersing TiO_2-modified activated carbon in ethanol to create a slurry. Then, by allowing the TiO_2-modified activated carbon slurry to fully disperse in a solution of polytetrafluoroethylene (PTFE, 60%), the activated carbon was able to form a network of channels and deposit TiO_2 crystals at random intervals within its interior structures (Dong, et al., 2012a; Dong, et al., 2012b).

The materials should be mixed with a mass ratio between the activated carbon, cation electrode resin, and polytetrafluoroethylene of 6:1:1. Cation exchanger resins (IER) were deposited directly onto the capacitive activated carbon particles and polytetrafluoroethylene (PTFE) binders. IERs can be used to enhance structural integrity of rGO matrices for the electrode construction. Subsequent stirring and drying of the mixture at 80°C ensures formation of an amorphous paste. The paste can be rolled into a 0.5 mm film to be placed on current collectors as CDI electrodes. This method enables the fabrication of larger and thinner electrodes to maintain a high mass transfer and prevent compromises in structural integrity of the activated carbon electrodes. Using the technology outlined above, larger-scale bioreactors based on TiO_2-modified activated carbon electrodes might be constructed for demineralization of desalinated water.

2.7 Characterization of Particles

To properly analyze the performance of the TiO_2@AC:rGO electrodes, one first has to understand the crystalline structure of the majority of the particles in the mixture. As described by Bourikas, et al. (2014), the majority of the structures are formed according to the principles of anatase structuralization or rutile chemistry. The chief difference between these two kinds of crystals pertains to the bulk structure. Another TiO_2 phase is commonly referred to as Brucker, turned out not to be conducive to effective CDI experiments because of a lack of electrical conductivity.

Both anatase and rutile crystalline structures are made up of TiO_6 octahedra networks. Anatase, on the one hand, consists of conventional unit cells of four TiO_2 particles. Rutile structures, on the other hand, consist of unit cells containing merely two TiO_2 particles.

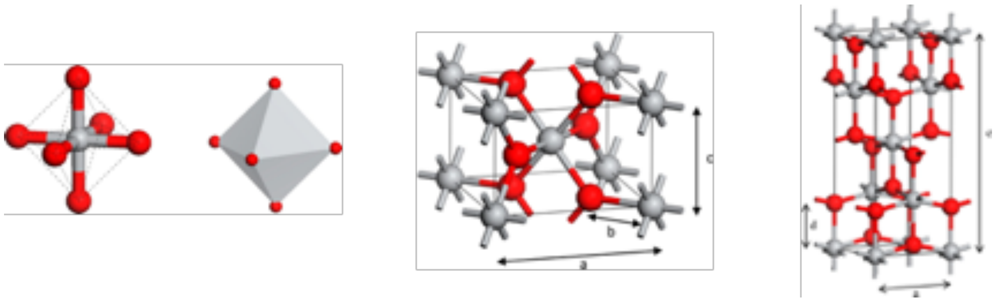

Figure 2.6.1: Schematic overview of Titanium oxide rutile (middle) and anatase (right) molecular structures based on TiO6 particles (left) (adapted from Bourikas, et al., 2014).

In both structures, each atom is engaged in one apical bond and two equatorial bonds. The difference matters because stacking, such as in graphite structures, is very different for anatase or rutile crystals (Bourikas, et al., 2014). Whereas in anatase structures, each octahedron is assembled in a network of eight octahedra where four share an edge and four share a corner, rutile structures conactivsist of networks of ten octahedra, where two share oxygen pairs and eight share single nuclear oxygen atoms (Chen and Mao, 2007).

2.8 Performance Evaluation

To evaluate the demineralization performance of the TiO_2@AC:rGO electrodes, single-salt (NaCl, 15mL, 1 M) experiments were conducted to determine the cation adsorption capacity at saturation (Ding, et al., 2019). Three samples of 100 mL of 0.5, 1.0, 1.5, 2.0 and 3.0 mM stock solutions were prepared. The notion at the basis of this examination was that competition between ions of different charge or size will likely decrease the adsorption of any ion and a measure of this decrease is useful in understanding how competitive adsorption works (Leong & Yang, 2019). The quantification of cation removal would determine the evaluation of the TiO_2@AC:rGO electrodes' efficacy in water demineralization.

The optimal demineralization performance for boron is best tested using a combination of standardized test solutions. Seen as this experiment focuses on the use of activated carbon and graphene-oxide composite materials for MCDI-based water demineralization, selective desalination to remove divalent ions such as sulfates and calcium ions will have to be examined for effective boron removal as well (Lhassani, et al., 2001). Selective removal is ideally achieved through a combination of nano filtration, while borates and nitrates are removed through electrodialysis (Lhassani, et al., 2001).

Adsorption capacity for activated carbon has traditionally been correlated to micropore and mesopore surface area. Earlier experiments, executed by Köse, et al. (2011) also highlighted the importance of having porosity of minimally 803 $m^2 g^{-1}$ at micropore volume to achieve the optimal demineralization capacity. The setup in the image below is representative of the basic nano filtration-electrodialysis hybrid setup for demineralization.

To evaluate the energy consumption and recovery of the TiO_2@AC:rGO electrodes, the test rig was connected to a potentiostat throughout the single-salt experiments to complete the two-electrode system. The current was measured by the potentiostat throughout the process. As described in the experiment by Han, et al. (2015), The MCDI cell was charged using a constant current. The current density was computed by dividing the total current by the projected area of the electrodes' surfaces (Han, et al., 2015). The MCDI cell was discharged by reversing the direction of the current upon completion of the single-salt experiment. The potentiostat would register when the total charge of the cell was at 0 V.

Qu, et al. (2016) assessed the energy consumption of an electrochemical cell based on the performance of AC induction in the system. The respective system measures the current needed for optimal desalination performance in a simple filtration MCDI setup. By effectively over-simplifying the demineralization process, the assessment of energy consumption is solely based on electrode performance. Due to the energy recovery possible because of pressure recovery in many reverse osmosis plants, the energy required to maintain the flow virtually becomes irrelevant in assessing the MCDI unit’s energy consumption.

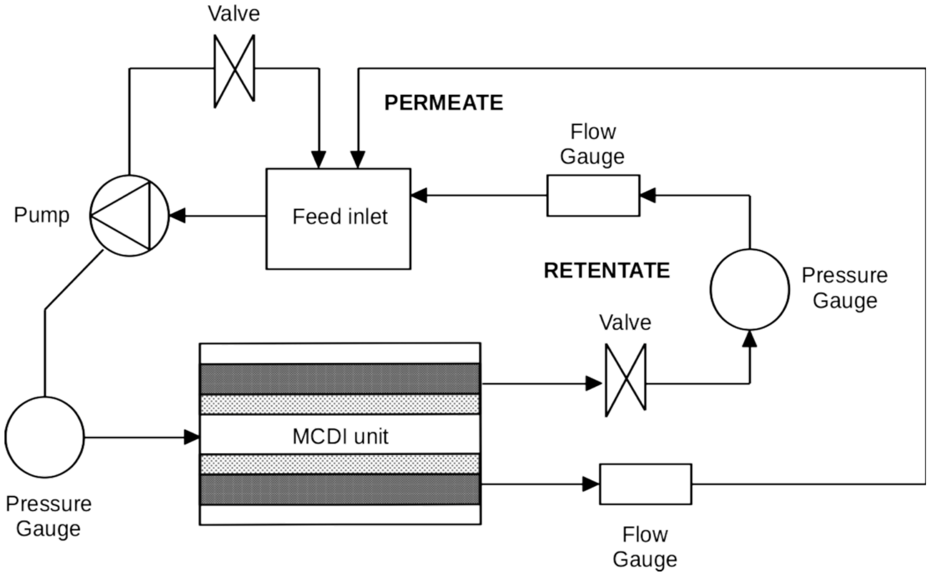

Figure 2.7.1: Schematic overview of nano filtration-electrodialysis combined activated carbon graphene-oxide composite material demineralization assessment (from Lhassani, et al., 2001).

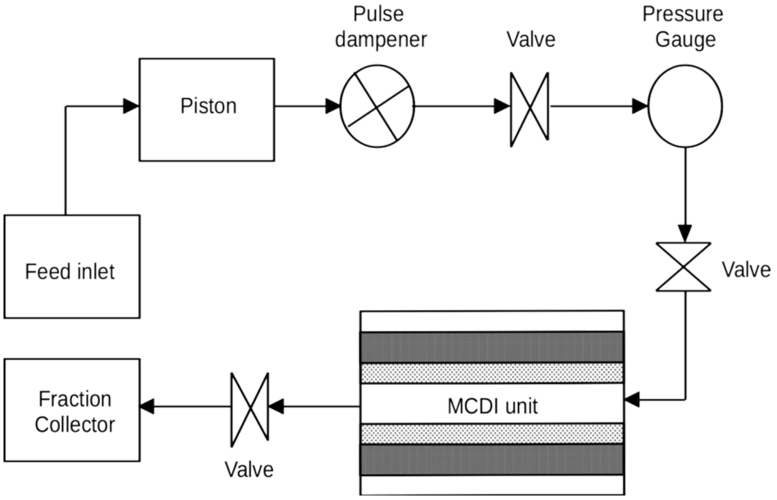

Figure 2.7.2: Schematic overview of monodirectional flow setup for energy consumption and recovery of MCDI electrodialysis and filtration testing (from Qu, et al., 2016; Kelley, et al., 2017).

Chapter 3

Experimental

The findings in this study were based on reduced graphene-oxide composites filled with functionalized activated carbon modified with TiO_2 crystals on its surface structures, more briefly referred to as TiO_2@AC:rGO.

All chemicals used in the study were of analytical grade. The reagents used in the preparation, including 3-aminopropyl)triethoxysilane (APTES, 99%), polyvinylidene difluoride (PVDF, 180K GPC) acetylene black and N-methyl-2-pyrrolidone (NMP, 99.5%), acetone (99%), acetic acid (99%), nitric acid (70%) and HCl (37%) were obtained from Sigma-Aldrich. The main precursor for TiO_2, titanium butoxide (97%) was also obtained from Sigma-Aldrich. Activated carbon (YP-80F) was purchased from Kuraray Co. Ltd. and water was used from Sartorius' Arium Pro UV machine. Commercial GO water dispersion was obtained from Graphenea.

3.1 Material Synthesis

First, animated AC was prepared using the method described by Xing, et al. (2016) and Leong and Yang (2019). The as-received AC was boiled in pure water at 100°C for two hours before fabrication to ensure any remaining contaminants from industrial production were removed. The boiled AC was dried in a dry oven at 60°C before use. Approximately 300 mg of AC was emulsified with 2.5 mL of APTES dissolved in acetone. The mixture was stirred at 70°C for 12 hours to ensure all acetone evaporated.

Second, the sol-gel method as originally described by Brinker and Scherer was then used to synthesize TiO_2@AC composite materials (Brinker & Scherer, 1990). A volume of 10 mL titanium butoxide ($Ti(OC_4H_9)_4$) dissolution was mixed with 34 mL of anhydrous ethanol and 2.5 mL of acetic acid under continuous stirring. The depositing mixture was created by diluting 17 mL anhydrous ethanol in 3 mL pure water and lowering the pH to 2-3 by adding diluted nitric acid.

The TiO_2 solution was generated by slowly adding the two mixtures together while stirring them at high rpm to produce dissolved TiO_2. The solution was mixed with the AC and stirred for a duration of 20 hours without light and at a temperature of 25°C in order to create AC consistently coated by the TiO_2 solution. The TiO_2@AC was subsequently washed with isopropyl alcohol to remove any remaining chemicals. The solid AC was deposited by repeated centrifugation for a duration of 5 minutes at the most. The final TiO_2@AC was dried at a temperature of 110°C for four hours.

Thirdly, the as-received GO water suspension was reduced by lowering to pH 11 to mimic natural, alkaline hydrothermal reduction mechanisms (Zheng, et al., 2017; Mei, et al., 2015). Water-emulsified GO was prepared by dissolving graphene-oxide suspension in 2M NaOH solution until pH value 11 was reached. After continuous stirring was maintained for some time, 40 mL of aqueous GO solution was heated to 180°C for 30 minutes to achieve optimal molecular bonding among the graphene-oxide matrix network. The rGO was then dried 90°C for 24 hours in a vacuum oven, together with the TiO_2@AC.

3.2 Electrode Fabrication

The electrodes were generated using the method for three-dimensional graphene composites as structured activated carbons for capacitive desalination described by Leong, et al. (2019). 300 mg of TiO_2@AC was mixed with PVDF and acetylene black in ratios 8:1:1. rGO and TiO_2@AC mixture were combined in equal ratios (1:1) and ground down to pure powdered form.

For correct deposition onto graphite paper for optimal (re)charging and decharging, a sludge was created in line with the method described by Brycht, et al. 3 mL of NMP were added to the mixture to create sludge. The powder and NMP were mixed in a mortar with a pestle for about 15 minutes to ensure the formation of a uniformly wetted paste. To enable complete homogenization, the paste was contained and left unused for 24 hours upon mixing. After this period had elapsed, the paste was deposited onto graphite paper of average thickness 0.5 mm by roll-pressing the paste onto the graphite material in equal measure. The depositions were dried in a drying oven at 90°C for 12 hours, ensuring optimal molecular bonding between the AC and the rGO for optimal electrode efficiency.

Chapter 4

Data Collection

After the TiO_2@AC:rGO composite electrodes were fabricated, the electrodes were characterized for surface functionalities, dispersion of crystallinity and overall AC-rGO bonding capacity. The two parts were characterized using X-ray and electron-microscopy technologies individually, and the combined TiO_2@AC:rGO composite material was quantified for demineralization performance.

4.1 Particle Characterization

The TiO_2@AC:rGO was characterized for surface functionalities by way of a field-emission scanning electron microscopy (FESEM, JEOL JSM-7600), as described by Ding, et al. (2019). The crystallinity and phases were analyzed using using powder X-ray diffraction (XRD, Bruker D8 Advance diffractometer) equipped with a Ni filtered Cu Kα radiation (λ = 1.5406 Å, 40 kV, and 40 mA) and by X-ray photoelectron spectroscopy (XPS, PHI-5400) with an Al Kα beam source (250 W). The corresponding chromatogram was compared to various earlier samples generated by Aneja, et al., Darvishi and Seyed-Yazdi, Wang, et al., and Yoon and Park to validate success of the AC generation process. The results were interpreted using CasaXPS software.

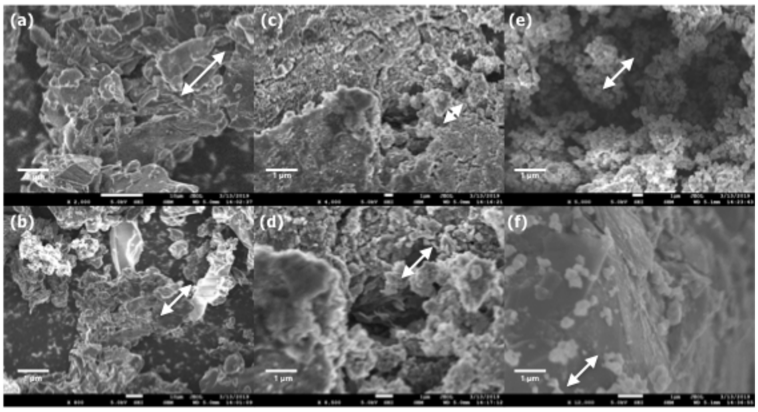

Figure 4.1.1: SEM imaging. (a) Overall AC structure. (b) Detailed AC structure. (c) Overall rGO structure. (d) Detailed rGO structure. (e) Overall TiO_2@AC structure. (f) Overall TiO_2@AC structure showing exact surface functionalities.

4.2 Crystallinity

To properly analyze the performance of the TiO_2@AC:rGO electrodes, the crystalline structure of the majority of the particles in the mixture has to be mapped. In TiO_2 surface chemistry, the majority of the particles in the mixture consist of a combination of rutile and anatase crystalline structure (Bourikas, et al. 2014). Anatase and rutile crystalline structures are made up of TiO_6 octahedral network modes. However, while anatase structures consist of conventional unit cells of four TiO_2 particles, rutile structures consist of dipolar TiO_2 particles (Chen and Mao, 2007). The majority crystalline structure will determine how graphite structures stack around the crystals in the electrode (Bourikas, et al., 2014).

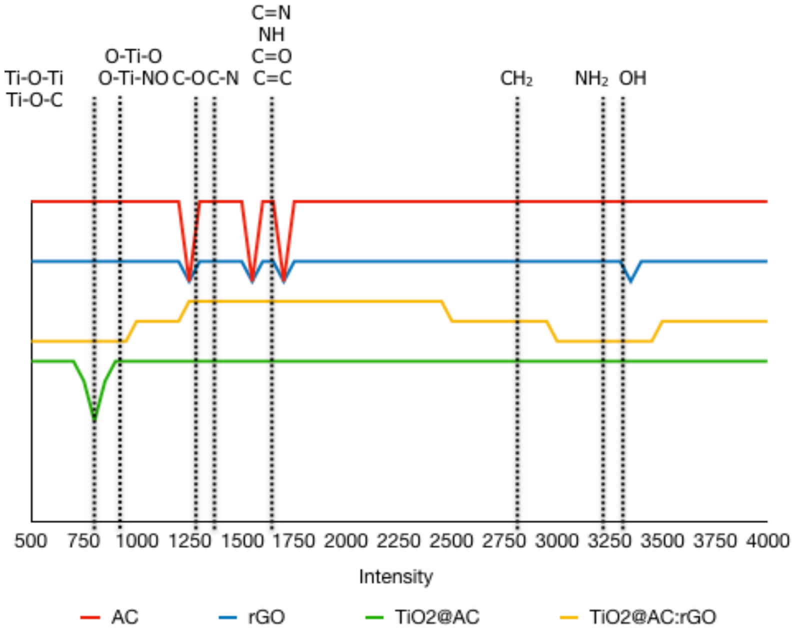

Figure 4.2.1: Photospectrometric Raman characterization.

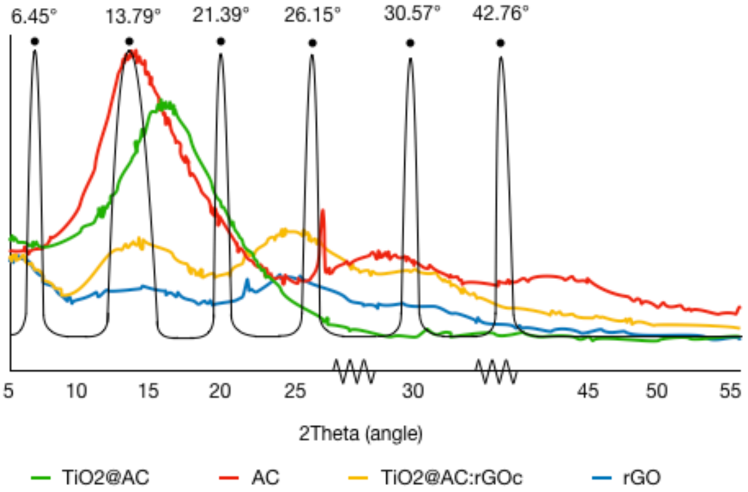

Figure 4.2.2: XRD images of APTES-AC, rGO and TiO_2@AC.

The X-ray diffraction tests showed peaks of varying intensity at angles ranging from 13.79° up to 36.57° (with higher peaks at 21.39° and 26.15°). Although the imaging results were somewhat distorted due to the relatively small quantity of viable sampling due to 2D graphene-oxide stacking, the peaks at 13.79° and 26.15° showed sufficient spread of crystallinity across the activated carbon architecture (Aneja, et al., 2015; Darvishi & Seyed-Yazdi, 2016; Wang, et al.. 2017; Yoon & Park, 2018). These angles also showed that there was an unequal combination of anatase and rutile crystals across the surface, showing that as expected from the earlier data review, the formation of crystallinity is largely uncontrollable across the surface of the matrix. For better quantification of which crystals are better for water demineralization, further research into tuning the crystal formation will have to be performed.

Comparing these results with the earlier Raman photospectrometry characterization showing Ti–O, Ti–C and Ti–NO bonds across the samples with TiO_2@AC indicated sufficient spead of TiO_2 crystallinity across the protein filler matrix connected to the AC filler. Although there were significant problems with graphene-oxide stacking in the filler-matrix architecture of the electrodes during fabrication, the SEM imaging showed that the crystals were visible on top of the architecture as well as in the AC-filler pores. The NMP protein treatment during fabrication was likely a significant contributor to the success of the formation of these surface functionalities.

4.3 Electrode performance quantification

To properly evaluate the demineralization performance of TiO_2@AC:rGO composite electrodes, the performance must be compared to benchmarking data available from previous studies. The experimental data reviewed in this paper was interpreted using previous work by Aneja, et al. (2015), Darvishi and Seyed-Yazdi (2016), Wang, et al. (2017), and Yoon and Park (2018).

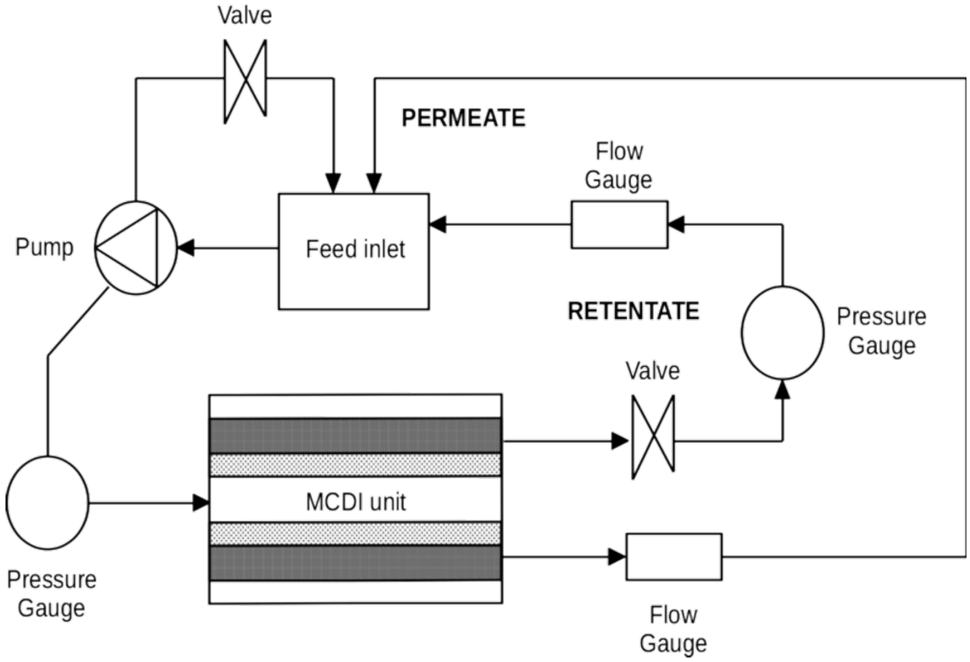

Figure 4.3.1: Experimental setup of water demineralization using a mechanical pressure-system to push water through the MCDI unit and back into the pump (adapted from Han, et al.).

Demineralization Performance. The examination of B^+ demineralization capacity should ideally be composed of standardized tests. Based on previous work by Lhassani, et al. other cations such as Na^+ can function in lieu of positively charged B^+ in solution. In this experiment, the demineralization performance of TiO_2@AC:rGO composite electrodes with polymer ion-exchange membranes will be examined using a single-salt Na^+ solution (NaCl, 15 mL, 1M). The relatively high molarity of this solution also helped assess the cation adsorption capacity at saturation after approximately 20 cycles (Ding, et al., 2019). The removal of divalent ions such as sulphates and Ca^{2+} requires more complicated saline solutions and will hence be studied in a separate study (Köse, et al., 2011). From the 1M stock, 150 mL solutions of 500 ppm, 1000 ppm and 1500 ppm NaCl were formulated for the demineralization performance experiments.

Before commencing the demineralization experiments, the TiO_2@AC:rGO composite electrodes were first washed with clean water for a duration of approximately two hours to wash out any remaining NMP and PVDF from fabrication to ensure optimal electrode conductivity. TiO_2@AC:rGO composite electrodes with AC:rGO mass ratio 1:1 and 1:2 were generated and benchmarked for water demineralization at a constant current of 0.3 V for a solution of 500 ppm NaCl, 1000 ppm and 1500 ppm NaCl solution. The conductivity and total dissolved solids (TDS) of the solitions were measured to determine the demineralization performance of 1:1, 1:2, 1:4 TiO_2@AC:rGO electrodes for a duration of seven demineralization cycles.

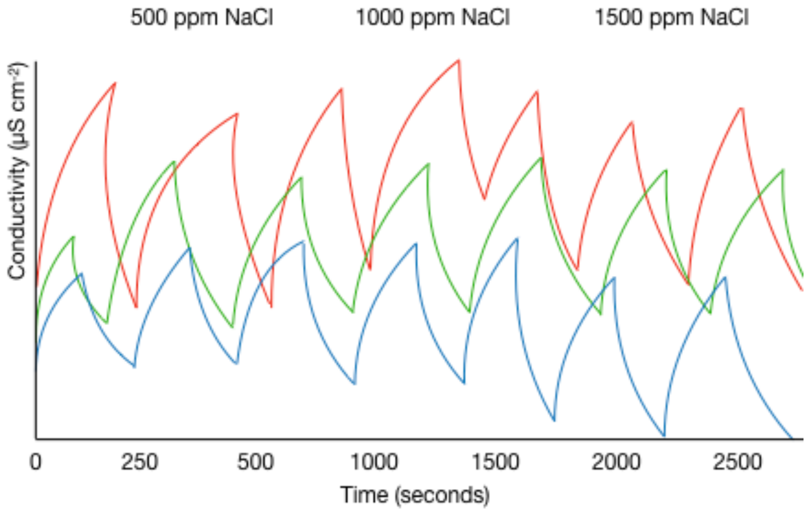

Figure 4.3.2: Demineralization performance for TiO_2@AC:rGO composite electrodes 1:1 AC:rGO mass ratio tested on (a) 500 ppm, (b) 1000 ppm and (c) 1500 ppm NaCl stock.

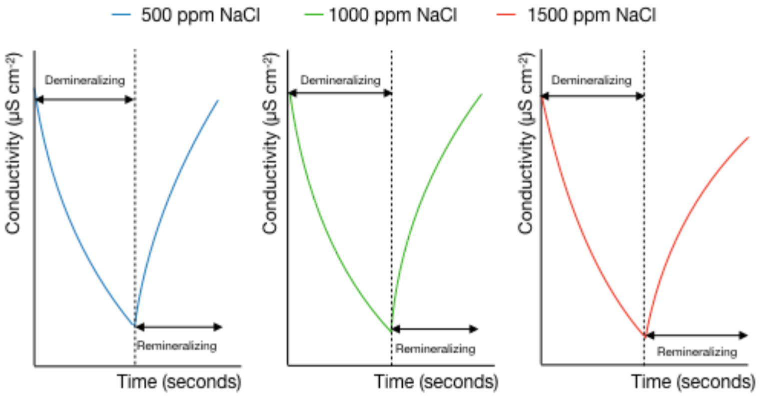

Figure 4.3.3: Demineralization and remineralization trends for TiO_2@AC:rGO composite electrodes 1:1 AC:rGO mass ratio tested on (a) 500 ppm, (b) 1000 ppm and (c) 1500 ppm NaCl stock.

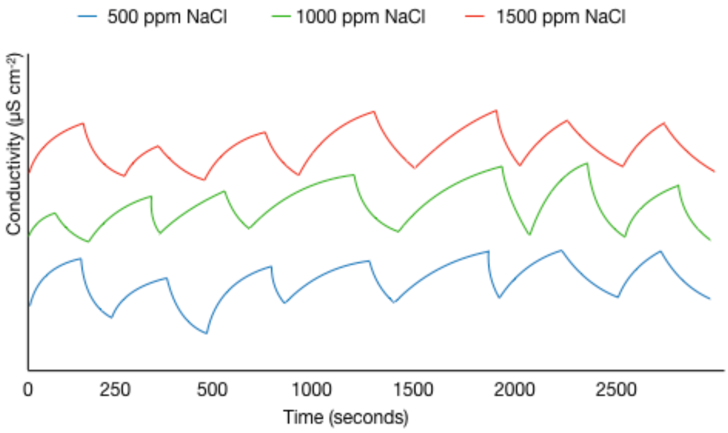

Figure 4.3.4: Demineralization performance for TiO_2@AC:rGO composite electrodes 1:2 AC:rGO mass ratio tested on (a) 500 ppm, (b) 1000 ppm and (c) 1500 ppm NaCl stock.

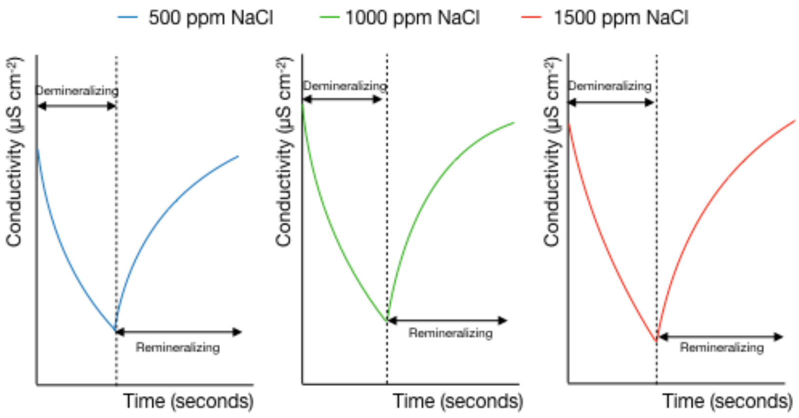

Figure 4.3.5: Demineralization and remineralization trends for TiO_2@AC:rGO composite electrodes 1:2 AC:rGO mass ratio tested on (a) 500 ppm, (b) 1000 ppm and (c) 1500 ppm NaCl stock.

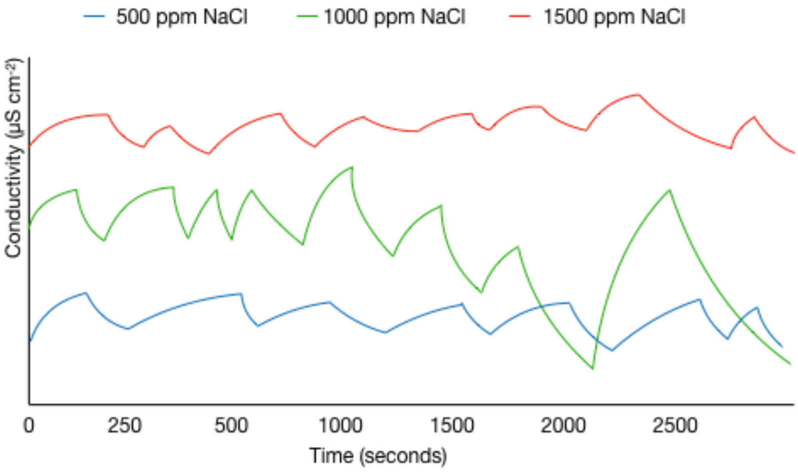

Figure 4.3.6: Demineralization performance for TiO_2@AC:rGO composite electrodes 1:4 AC:rGO mass ratio tested on (a) 500 ppm, (b) 1000 ppm and (c) 1500 ppm NaCl stock.

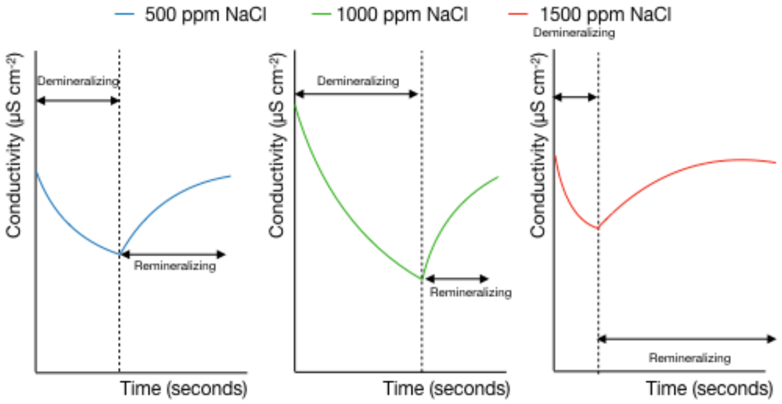

Figure 4.3.7: Demineralization and remineralization trends for TiO_2@AC:rGO composite electrodes 1:4 AC:rGO mass ratio tested on (a) 500 ppm, (b) 1000 ppm and (c) 1500 ppm NaCl stock.

The demineralization performance of the electrodes was tested using the degree of salt rejection relative to the remineralization levels after each cycle. The lower the level of remineralization compared to the initial salt concentration, the more effective the electrode was deemed to be at retaining demineralized salt in the porous matrix.

The remineralization levels were approximately equal for 1:1 TiO_2@AC:rGO and 1:4 TiO_2@AC:rGO mass ratio levels. Although the total demineralization performance of the 1:1 TiO_2@AC:rGO mass ratio electrodes seemed to be more effective, for 500 ppm, 1000 ppm and 1500 ppm NaCl stock, the 1:2 TiO_2@AC:rGO mass ratio electrodes seemed to have less significant remineralization compared to the initial demineralization rate. Further testing is required to optimize the mass ratio for matrix distribution and conductivity to attain optimal desalination effect.

The majority of the more effective electrode mass balances, the salt rejection levels remained relatively low, at approximately 2–4% of the total initial salt concentration after 20,000 seconds. The total salt rejection in the earlier cycles of the 1:1 TiO_2@AC:rGO mass ratio electrodes topped out at 7% of the total initial salt concentration. The maximum concentration of 541 ppm NaCl was lowered to 508 ppm at the second cycle of the first test. Future testing is required to optimize the conductivity of the electrode matrices to attain better demineralization performance.

In summary, the slight difference in electrosorption with increasing levels of rGO in fabrication mixture decreased the conductivity of the electrodes overall. The equal dispersion of the AC filler in the rGO matrix made that the conductivity could be optimized per mass ratio whilst maintaining the total level of structural integrity from the 2D rGO architecture. Future testing will have to be applied to optimize the conductive filler in the structurally integral rGO matrix.

Electrical conditions for demineralization performance. The demineralization trials were run at constant voltage of 0.3 V using a Keithley 2450 SourceMeter® — a source measure unit (SMU) instrument that is ideal for current measurement at low-voltage operations due to its current measurement limitation of 1 A. Previous studies suggested that maintaining constant voltage and variable current would aid best in quantifying the progression of the decrease of demineralization efficiency over time (Han, et al., 2015; Ding, et al., 2019; Kim, et al., 2017; Leong & Yang, 2019). The results must hence be interpreted as a small-scale exaggeration of the real-life context. This study aims to exhibit a proof-of-concept with regard to the viability of TiO_2@AC:rGO composite electrodes for water demineralization purposes. The demineralization performance of saline solutions of 500 ppm, 1000 ppm and 1500 ppm were examined under the same electrical conditions for optimal reference data.

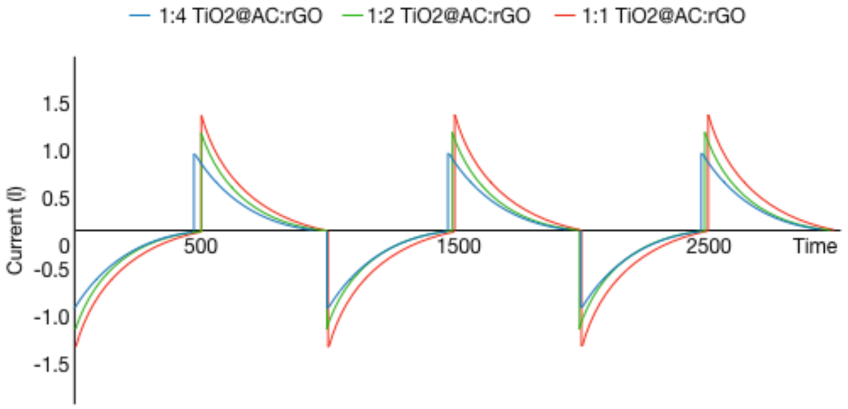

Figure 4.3.8: Energy adsorption and resorption patterns for TiO_2@AC:rGO composite electrodes (a) 1:1 AC:rGO mass ratio, (b) 1:2 AC:rGO mass and (c) 1:4 AC:rGO mass ratio ratio tested on 500 ppm, 1000 ppm and 1500 ppm NaCl stock.

The study aimed to show the changes in electrosorption with increasing mass ratios in the rGO matrix of the electrodes would steadily increase the structural integrity of the electrodes. The challenge was to find optimal mass ratios for the activated carbon filler to be able to support the same conductivity and maintain electrosorption capacity in different configurations. The graph of the electrosorption pattern confirmed that even though slight decreases in AC content with increasing rGO concentration would support the same kind of electrosorption patterns.

Chapter 5

Conclusions

Upon assessment of the SEM images, the activated carbon porosity was determined to seem relatively equally dispersed across the surface. Similarly, the reduced graphene oxide was stacked and showed sufficient porosity. As assumed from the photospectrometric imaging, the TiO_2 surface functionalizations were indeed equally dispersed across the surface and even filled up the majority of the places inside the pores. The XRD and Raman spectra of the samples showed an equal dispersion of rutile and anatase crystalline structures. However, the location of these peaks seemed to be little controllable. As a consequence, there might be little opportunity to tune the prevalence of each of these structures and hence the ability to measure their effectiveness for water demineralization capacity might be limited.

The water demineralization performance for TiO_2@AC:rGO composite electrode materials were assessed for 1:1 TiO_2@AC:rGO ratio, 1:2 TiO_2@AC:rGO mass ratio, and 1:4 TiO_2@AC:rGO mass ratio. Based on literature assessment, this work suggested that the higher the degree of GO, the better the dispersion of available TiO_2 contact areas for demineralization would be. However, the results showed that the demineralization performance of 1:1 TiO_2@AC:rGO ratio was much more efficient than 1:2 or 1:4 TiO_2@AC:rGO ratio.

During the reduction of GO, the tendency was determined to stick together in singular layers and clog pores. Only by mixing the GO with the AC before completing the reduction cycle, a sufficiently consistent dispersion of pores was created. However, in higher amounts of GO, this method might not have sufficed to prevent clogging. The demineralization tendencies, however, definitively show that the electrodes with TiO_2@AC:rGO ratio 1:1 were much more efficient in demineralization performance.

The energy performance for the 1:1, 1:2 and 1:4 TiO_2@AC:rGO composite materials were also assessed. The results showed that while the two composite materials showed virtually the same charging and recharging patterns in the first couple of phases, the 1:2 and 1:4 TiO_2@AC:rGO composites eventually showed a significantly decreased ability to decharge, maintaining a certain level of electrical charge at all times. The increased degree of rGO semiconductor in the matrix might have led to a decreased totality of the carbon conductivity, maintaining charge and decreasing the overall charging capability.

Based on the charging and recharging performance assessed, the energy consumption behavior of the materials at a larger scale might be speculated upon. While the 1:2 and 1:4 TiO_2@AC:rGO electrodes showed significantly less energy consumption for the performance assessment, and the current recovery was greater, this might have been due to the electrical current stored in the electrodes due to the decreased conductive mesh. As the demineralization performance of the 1:2 and 1:4 TiO_2@AC:rGO electrodes was not satisfactory, however, the further exploration of the reason for its better energy recovery is not the best performance testing for the purposes of this work.

Chapter 6

Recommendations

Based on the literature review conducted prior to this study, this report concludes that optimally to reduce the energy consumption of water demineralization devices, the necessity for artificial pressure generation should be reduced. Especially in the case of Singapore, the current energy consumption of the NEWater systems, largely based on ultrafiltration and reverse osmosis, equates to approximately 3.5 kWh per meter cubed of potable water generated, according to Singapore's Public Utilities Board (Chong Mien Ling, personal communication, February 22, 2019). Furthermore, removal of cation such as calcium and boron is difficult because these ions need to be removed at a pH of approximately 10.5, requiring further remineralization upon completion of the water treatment process (Chong Mien Ling, personal communication, February 22, 2019). As a result, to bring down the energy consumption of these pressure-based processes to less than 1.0 kWh per meter cubed of freshwater generated, with a boron concentration of less than 0.5 ppm, alternative membrane-based processes will need to be explored.

Furthermore, according to reports by PUB, the climate is changing the frequency of monsoons. Combined with the shortage of surface area for rainwater catchments in Singapore, this leads to a need for alternative water provision. To address the increased need for wastewater treatment for ions impacting health, water recycling using electrochemical demineralization technologies need to be explored in further detail.

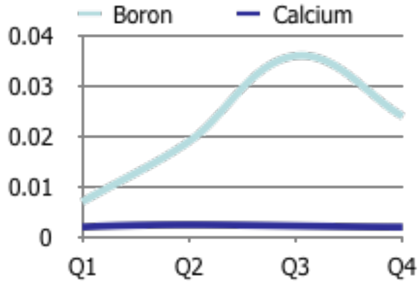

Figure 6.0.1: The increase in average concentration of calcium and boron cations in wastewater in Singapore between the first and fourth quarters of 2018 (adapted from pub.gov.sg, 2018).

6.1 Wastewater Recycling in Singapore

Currently, Singapore generates 60% of its water using the NEWater wastewater recycling system (Esther Tan, personal communication, February 22, 2019). The majority of this wastewater comes from Johor Bahru, Malaysia, Singapore households and industry. This water is guided along a sloped tunnel system into just five wastewater treatment facilities in the city. Over the course of water treatment in the NEWater program, water is pretreated chemically, microscopic particles are filtered out using microfiltration, undesirable contaminants are removed using reverse osmosis, and any remaining pathogenic particles are treated using ultraviolet disinfection (pub.gov.sg, 2018).

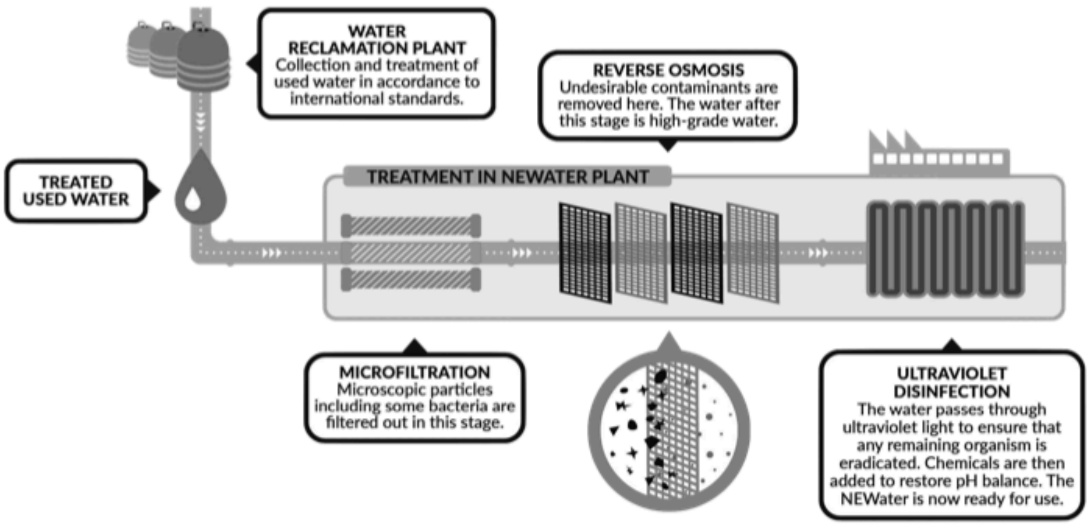

WATER RECLAMATION PLANT
Collection and treatment of used water in accordance to international standards.

REVERSE OSMOSIS
Undesirable contaminants are removed here. The water after this stage is high-grade water.

MICROFILTRATION
Microscopic particles including some bacteria are filtered out in this stage.

ULTRAVIOLET DISINFECTION
The water passes through ultraviolet light to ensure that any remaining organism is eradicated. Chemicals are then added to restore pH balance. The NEWater is now ready for use.

Figure 6.1.1: Simplified overview of microfiltration and reverse osmosis in Singapore's NEWater facilities for wastewater treatment (adapted from pub.gov.sg, 2018).

The main requirement for mechanical filtration and reverse osmosis is the generation of mechanical pressure to push the water through the active membranes for treatment (Rovel, et al., 2003; Song, et al., 2012; Shon, et al., 2013). In mechanical filtration, such as microfiltration, water is pushed down, whereby the net pressure pushes the water through the semipermeable membrane in the middle of two chambers, leaving the saline particles behind and only filtering through clean water without coions. In reverse osmosis, mechanical pressure is applied to push the water through the membrane linearly, leaving behind any coions before the membrane.

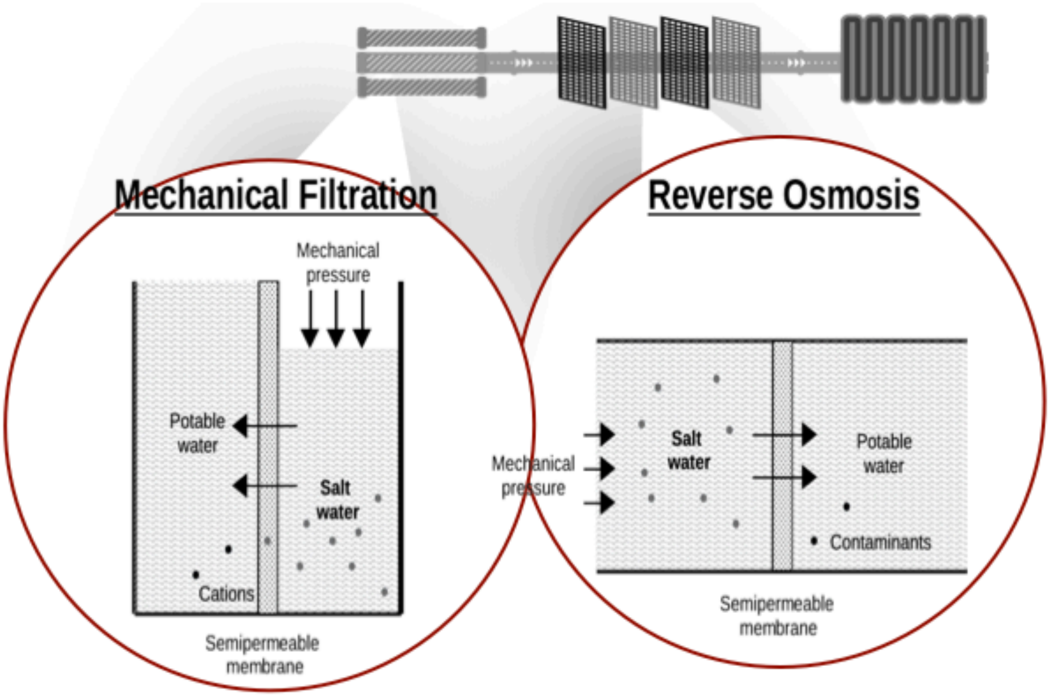

Figure 6.1.1: Mechanical filtration and reverse osmosis-based desalination technologies based on mechanical pressure generation (adapted from Rovel, et al., 2003; Song, et al., 2012; Shon, et al., 2013).

6.2 Mathematical Modeling

According to Gabelich, et al. (2012), the alternative electrochemical method of membrane-based capacitive deionization (MCDI) is an effective electrochemical water demineralization technique that requires solely electrical energy. Additionally, though the use of a so-called desalination battery, storage of electrical energy in coionic bonds in the saline solution, energy recovery helps further reduce the total quantity of electrical energy required for the device to function (Gabelich, et al., 2002). However, as this technique can function largely without artificial pressure generation, and using natural water surface pressure, the scalability of this technology has so far been limited (Gabelich, et al., 2002).

After careful consideration of the system limitations, the inflow mass transfer was determined by the power in the system (W), the length of the chamber (L) and the flux of the system (Jv). Using the equation below, the total water quantity in the system for each coil configuration was computed. The flux of the system was determined using the surface area of the electrodes, the pressure difference in the system, and the total concentration of the saline solution run through the system.

$$Q_p = n_l\ W \int_0^L J_v\ dt = (Q_f - Q_r)\ \Delta t \qquad \text{(Eq. 1)}$$

$$J_v = A\ \Delta P - A\ RT\ (C_f - C_p) \qquad \text{(Eq. 2)}$$

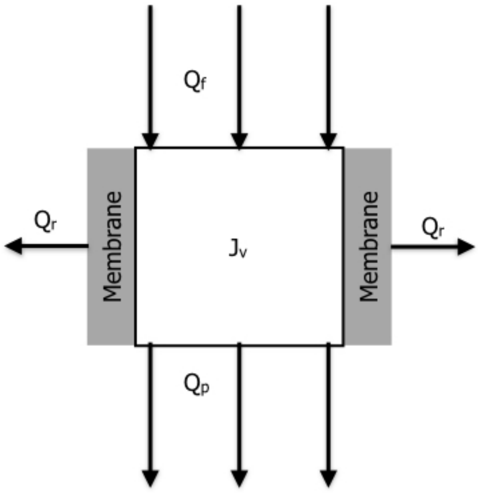

Figure 6.2.1: Flux and inflow mass-based water desalination (adapted from Al-Shayji & Liu, 2002; Jiang, et al., 2014; Garcia-Aleman, 2002).

In the equation describing the mass balance of water, Q_p is the pressurized mass of water flowing through the system in kg; n_i is the number of particles in the system; W is the force exerted on the water quantity in N m; L is the maximum length of the system in m; J is the flux in the system in mL L^{-1}; Q_f is the desalinated mass of water in kg and Q_r is the mass of the retentate after desalination in kg, with Δt being the difference in time throughout the system in seconds.

In the equation describing the flux, J is the flux in the system in mL L^{-1}; A is the surface area of the electrodes in m^2; ΔP is the pressure difference between the liquid masses in the system in Pa; R is the universal liquid constant; T is the temperature of the system in K; C_f is the initial concentration of saline solution before desalination in mg L^{-1} and C_p is the concentration of saline solution after desalination in mg L^{-1}.

When observing a cylindrical system, the water is guided along the walls of the electrodes at an angle, and the pressure difference becomes a forward force. The pressure difference is determined using the differential pressure with the angle between each of the coils.

$$Q_p = n_l \, \Delta P \tan\theta \int_0^L J_v \, dt = (Q_f - Q_r) \, \Delta t \qquad \text{(Eq. 3)}$$

$$J_v = A \, \Delta P \tan\theta - A \, RT \, (C_f - C_p) \qquad \text{(Eq. 4)}$$

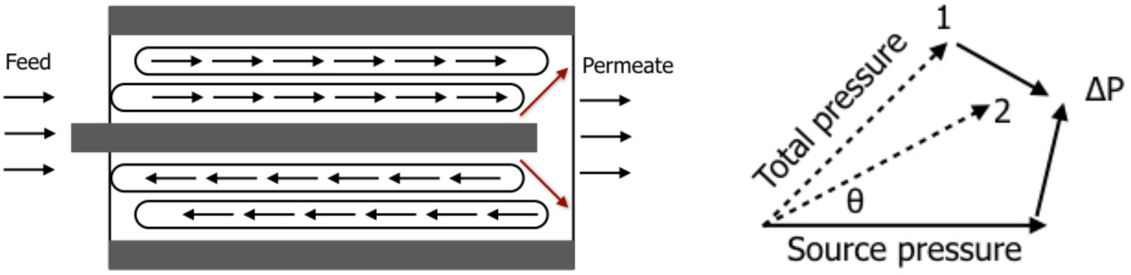

Figure 6.2.2: Pressure flux in a cylindrical system, modeled based on the angle between the bidirectional pressure difference (adapted from Jiang, et al., 2014; Garcia-Aleman, 2002).

In the equation describing the mass balance of water, Q_p is the pressurized mass of water flowing through the system in kg; n_i is the number of particles in the system; W is the force exerted on the water quantity in N m; L is the maximum length of the system in m; J is the flux in the system in mL L^{-1}; Q_f is the desalinated mass of water in kg and Q_r is the mass of the retentate after desalination in kg, with Δt being the difference in time throughout the system in seconds.

In the equation describing the flux, J is the flux in the system in mL L^{-1}; A is the surface area of the electrodes in m^2; ΔP is the pressure difference between the liquid masses in the system in Pa; θ is the angle between the point of entry for the water flux and the stream through the system in degrees (°); R is the universal liquid constant; T is the temperature of the system in K; C_f is the initial concentration of saline solution before desalination in mg L^{-1} and C_p is the concentration of saline solution after desalination in mg L^{-1}.

The model explains how the pressure is converted into forward force using the change in angle. The closer the angle reaches to a constant θ of approximately 45°, the closer the tangent will be to maximizing the forward force from the pressure difference. The maximum flux in the system would be achieved can be achieved when the tangent is closer to one because of optimal pressure maintenance. The water should be cycled through the system in a circular motion to maintain this angle optimization.

Using a simplified, gravity-based cylindrical, coil-based desalination chamber with electrochemical TiO_2@AC:rGO composite membranes and ion-exchange membranes. The water enters the system through a vertical water inlet, is guided along internal coils maximized at an angle of approximately 45° for water flux optimization. The coils function as a spacer between the membranes angled at 45° throughout the system for optimal distribution of water along the electrodes, maintaining pressure conversion into forward force of water.

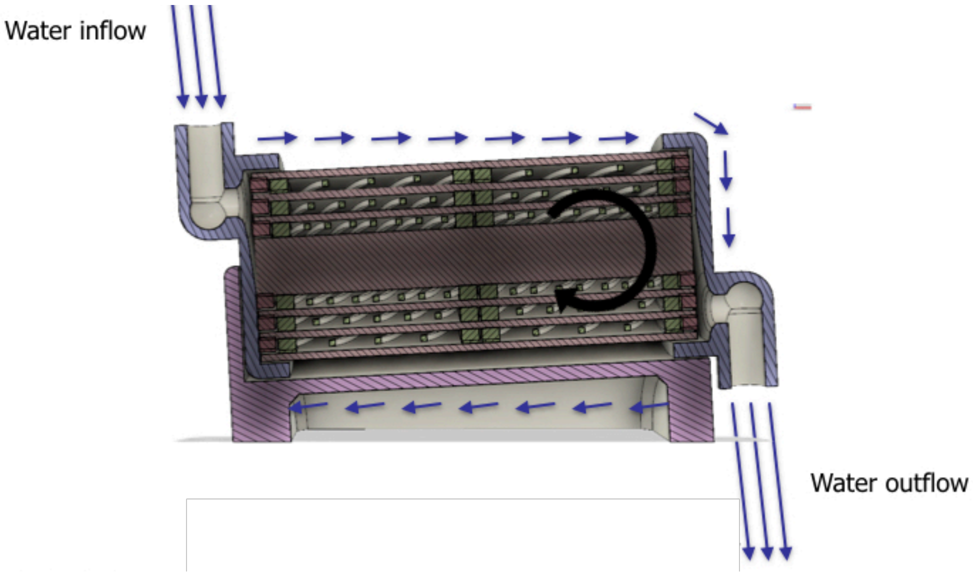

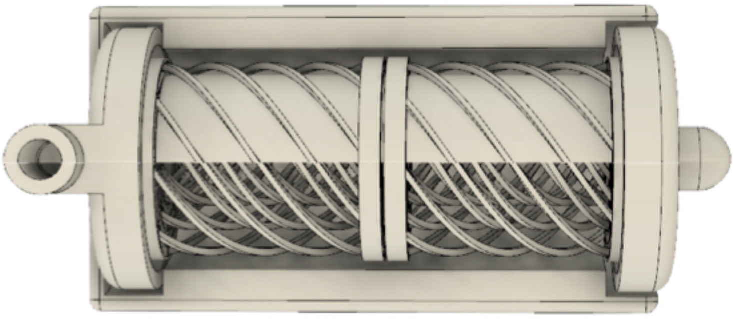

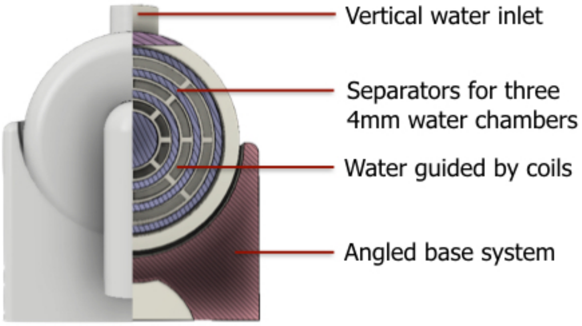

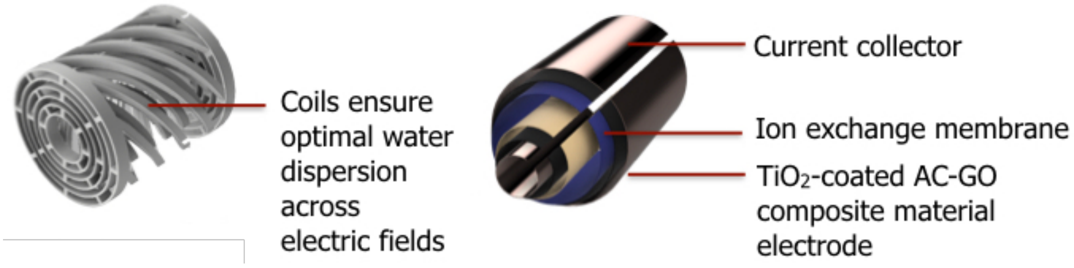

Figure 6.2.3: Internals of coil-based water demineralization device. Coils ensure optimal water dispersion across electric fields. Current collectors, ion-exchange membranes and electrodes are placed layered between the coils and spacers to ensure optimal dispersion of the saline water across the electrode.

The layout supports a vertical water inlet, leading into cylindrical chambers with separators of 4 mm between the electrodes and ion-exchange membranes. The water is guided by coils all positioned optimally at 45° from each other. This optimizes the tangent relationship between the bidirectional pressure generation from the water flow. Furthermore, the base of the system is placed at an angle to ensure the water at the bottom of the system flows back, maintaining the internal pressure and ensuring the device will continue to efficiently demineralize the water input.

The setup was tested using a simplified setup with a voltage meter, a current meter, a mobile power generator and a volume of 150 mL 500 mg per liter sodium cation solution run at a 1000 μS cm^{-2} for 20,000 seconds. Furthermore, the MCDI electrode was placed at an angle of between 5 and 15° on a flat surface both to minimize the number of changing variables in the test setup and establishing an increasing water demineralization efficiency for increasing angles at which the water is guided through the electrochemical system.

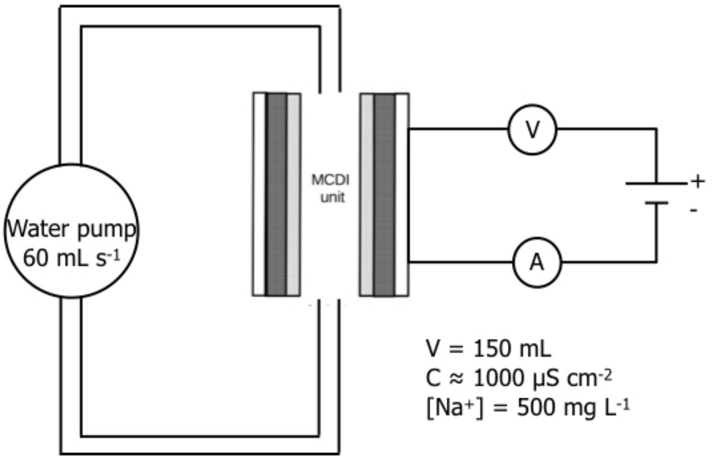

Figure 6.2.4: Simplified setup for angled water demineralization assessment. Two-dimensional water desalination test setup for angled examination.

After constructing the prototype desalination device, the desalination was tested for 500 ppm sodium solution at 5°, 10° and 15° angles using a 60.0 mL per second pressure pulse for construction feasibility. The results of the conductivity of the saline solution was assessed to establish the effectiveness of the angle-based approach to demineralization. To better assess the competitiveness of the technology, the adsorption capacity, the desalination battery charging and recharging patterns, and the energy consumption and recovery of the system were computed.

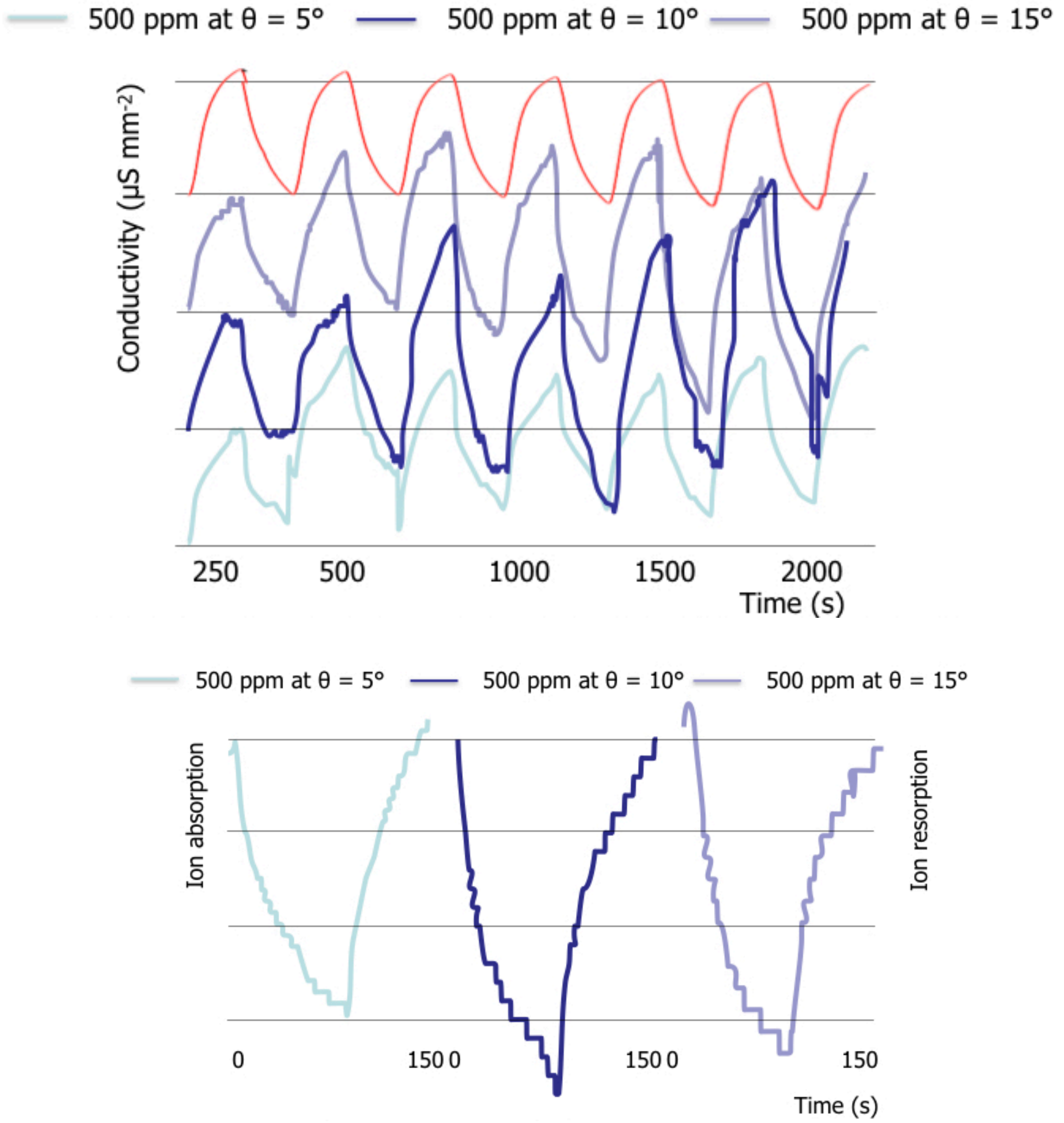

Figure 6.2.5: Conductivity for demineralization performance of angle-based desalination unit. The seemingly gradual decrease of the lower maxima of the demineralization performance show that the greater the angle, the higher the pressure, the more effective the total demineralization performance is across time.

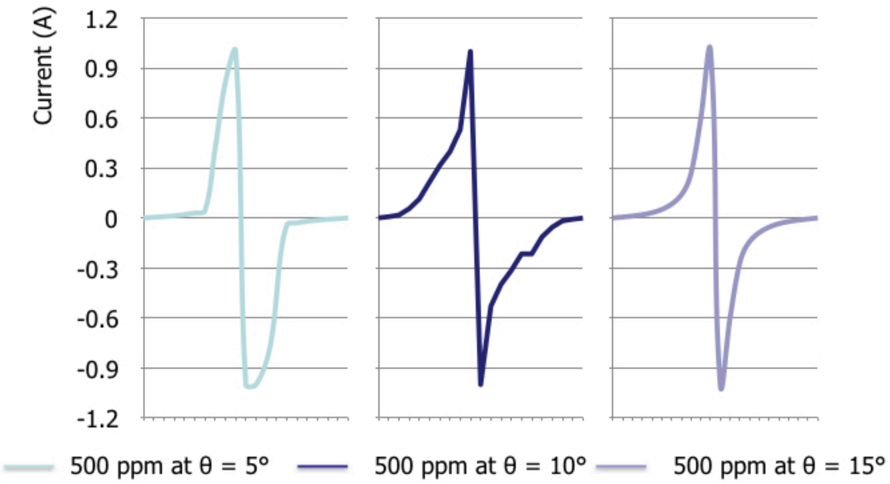

Figure 6.2.6: Desalination battery charging and recharging patterns.

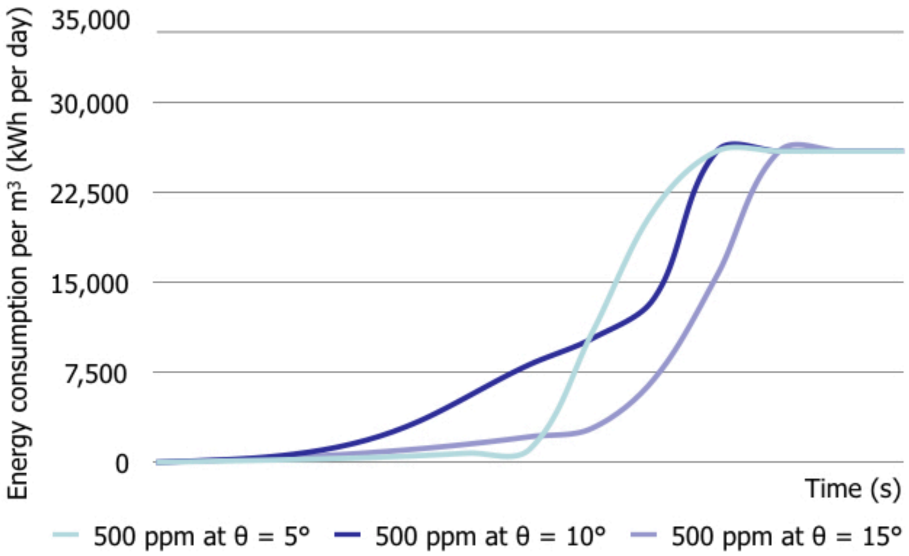

Figure 6.2.7: Projected energy consumption for the angle-based demineralization test at 45° compared with current technologies (adapted from Qin, et al., 2019).

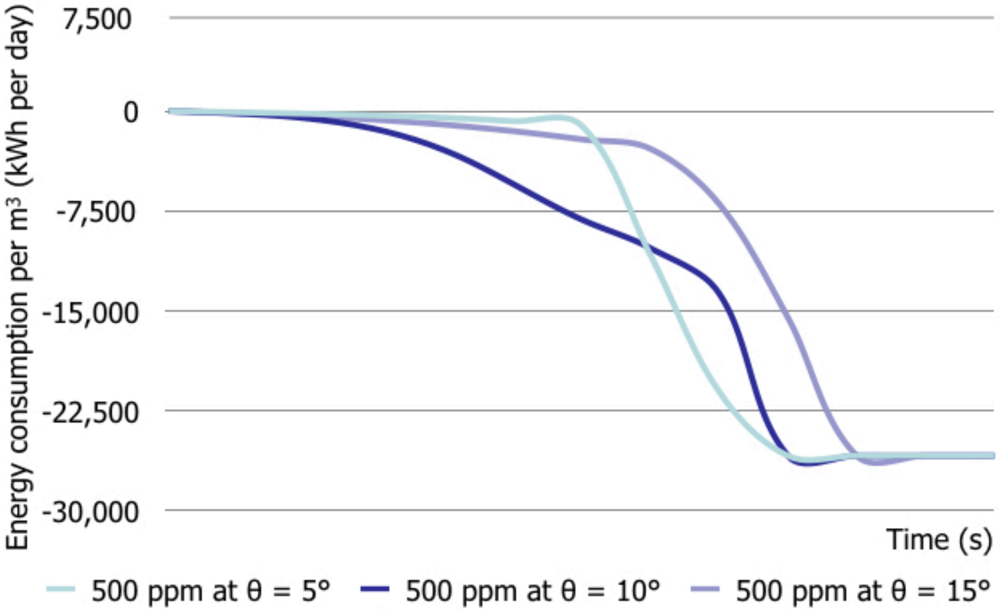

Figure 6.2.8: Projected energy recovery for the angle-based demineralization test at 45° compared with current technologies (adapted from Qin, et al., 2019).

Using demineralization tests of 500 ppm NaCl stock run at a constant voltage of 0.3 V for angles of 5°, 10° and 15° due to manufacturability considerations in small-scale models, the basic principle of improved demineralization performance at higher angles was shown successfully. The tests also show that the flux and demineralization capacity steadily increase with higher angles in the system. Similarly, the higher angles also showed smoother electrosorption patterns, presumably due to less water piling up in the ducts in the system.

By way of the electrosorption dynamics of Newtonian electronic principles, the projected maximum energy consumption throughout the 20,000 seconds of cycling water through the system, the maximum engery consumption tops out at approximately 2.5 kWh m^{-3}. However, due to the equal salt concentration being run through the system at repeated frequency, the results might be somewhat skewed. Future retesting using larger water volumes and lower saline concentrations is advised to find purer results.

Based on careful examination of the results for the design experimented on in this study shows the feasibility of angle-based demineralization with decreased energy consumption. The combination of energy recovery with solely using electrical energy could easily bring the energy consumption all the way down to close to zero. For future design solutions, the scalability would require a more extensive network of flow guidance, perhaps using different angles for energy storage and recovery in the desalination battery.

On a more theoretical level, the design still requires more research into the angles used to optimize water dispersion in the system. Currently, the system uses water retention at the bottom of the chamber to retain some of the internal pressure, effectively also limiting the demineralization performance. However, if the angles can be tuned to maintain a water pressure difference similar to the flow rate at the entry point, better water dispersion and flow through should be achieved, further enhancing demineralization performance.

Another point of attention is the energy recovery from the desalination battery. Based on the examinations by Jiang, et al. (2014) and Garcia-Aleman (2002), the energy consumption depends significantly on the efficiency of energy recovery from the desalination battery. However, in most systems, the energy recovery efficiency depends on the conductivity of the water and its ability to use this energy recovery for further improvement of the desalination performance.

Lastly, the current prototype was constructed of poly lactic acid, an easily malleable but not very durable type of plastic. Similarly, the use of this plastic prevented the construction of the intricate internal coil structure needed for optimal demineralization performance. Future designs should be constructed of more durable materials, particularly suitable for a variety of saline, temperate and tropical climates. Materials such as acrylonitrile butadiene styrene, or polyvinyl chloride would pose suitable candidates.

Bibliography

Ahadian, S., & Kawazoe, Y. (2009). *An artificial intelligence approach for modeling and prediction of water diffusion inside a carbon nanotube*. Nanoscale Resolution Letters, 1054–1058.

Agre, P. (2003). *Aquaporin Water Channels*, Nobel Lecture. Stockholm, Sweden.

Akbari, A., Sheath, P, Martin, S.T., Shinde, D.B., Shaibani, M., et al. (2016). *Large-area graphene-based nanofiltration membranes by shear alignment of discotic nematic liquid crystals of graphene oxide*. Nature Communications, 7: 10891.

Anderson, M. A., Cudero, A. L., & Palma, J. (2010). *Capacitive deionization as an electrochemical means of saving energy and delivering clean water. Comparison to present desalination practices: Will it compete?* Electrochemical Acta, 55, pp. 3845-3856.

Aneja, K.S., Bohm, S., Khanna, A.S., & Bohm, H.L.M. (2015). *Graphene based anticorrosive coatings for Cr (VI) replacement.*Nanoscale, 00, pp. 1–3.

Barakat, M. (2011). *New trends in removing heavy metals from industrial wastewater*. Arabian Journal of Chemistry, 4, pp. 361-377.

Brinker, C.J., & Scherer, G.W. (1990). *Sol-Gel Science: The Physics and Chemistry of Sol-Gel Processing*. Academic Press.

Brycht, M., Leniart, A., Zavašnik, J., Nosal-Wiercińska, A., Wasiński, K., et al. (2018). *Paste electrode based on the thermally reduced graphene oxide in ambient air – Its characterization and analytical application for analysis of 4– chloro–3,5–dimethylphenol*. Electrochimica Acta, 282(20): 233–241.

Bourikas, K., Kordulis, C., & Lycourghiotis, A. (2014). *Titanium Dioxide (Anatase and Rutile): Surface Chemistry, Liquid–Solid Interface Chemistry, and Scientific Synthesis of Supported Catalysts*. Chemical Reviews, 114(19): 9754–9823.

Buczek, B. (2016). *Preparation of Active Carbon by Additional Activation with Potassium Hydroxide and Characterization of Their Properties*. Advances in Materials Science and Engineering.

Carpenter, A.W., de Lannoy, C.F., & Wiesner, M.R. (2015). *Cellulose Nanomaterials in Water Treatment Technologies*. Environmental Science and Technology, 49(9): 5277–5287.

Chen, X., & Mao, S.S. (2007). *Titanium Dioxide Nanomaterials: Synthesis, Properties, Modifications, and Applications*. Chemical Reviews, 107(7): 2891– 2959.

Cotruvo, J.A. (2015). *Desalination Guidelines Development for Drinking Water: Background.*

Darvishi, M., & Seyed-Yazdi, J. (2016). *Microwave irradiation synthesis of TiO2/graphene nano-hybrid using titanium butoxide with enhanced photocatalytic activity.* Scientia Iranica F, 23(3): 1548–1553.

Das, R., Ali, E., Hamid, S.B.A., & Ramakrishna, S. (2014). *Carbon nanotube membranes for water purification: A bright future in water desalination*. Desalination, 336(1): 97–109.

Dey, D., Herzog, A., & Srinivasan. (2007). *Chemical Precipitation: Water Softening*. Department of Civil and Environmental Engineering, Michigan State University East Lansing, ENE, 806.

Ding, M. Fan, S., Huang, S., Pam, M.E., Guo, L., et al. (2019). *Tunable Pseudocapacitive Behavior in Metal-Organic Framework Derived TiO2@Porous Carbon Enabling High-Performance Membrane Capacitive Deionization.* [Not yet published].

Ding, M., Shi, W., Leong, Z., Guo, L., Baji, A., & Yang, H. Y. (2017). *Bimetallic Metal-Organic Frameworks Derived Porous Carbon Nanostructure for High Performance Membrane Capacitive Desalination*. Journal of Material Chemistry A, 5, pp. 6113-6121.

Długołęcki, P., & van der Wal, A. (2013). *Energy recovery in membrane capacitive deionization*. Environmental Science and Technology, 47, pp. 4904-4910.

Dong, H., Yu, H., & Wang, X. (2012a). *Catalysis kinetics and porous analysis of rolling activated carbon-PTFE air-cathode in microbial fuel cells*. Environmental Science & Technology, 46(23): 13009–13015.

Dong, H., Yu, H., & Wang, X. (2012b). *A novel structure of scalable air-cathode without Nafion and Pt by rolling activated carbon and PTFE as catalyst layer in microbial fuel cells*. Water Resources, 46(17): 5777–5787.

Drinking Water Quality: *Drinking Water Monitoring*. (2018). pub.gov.sg. Retrieved April 17, 2019, from https://www.pub.gov.sg/watersupply/waterquality/drinkingwater.

Dundorf, S., MacHarg, J., Sessions, B., & Seacord, T.F. (2009). *Optimizing Lower Energy Seawater Desalination: The Affordable Desalination Collaboration*, IDAWorld Congress, Dubai, UAE.

Efraty, A., Barak, R.N., Gal, Z., 2011. *Close circuit desalination — a new low energy high recovery technology without energy recovery*. Desalination Water Treatment, 31, pp. 95–101.

Entezari, M.H., & Tahmasbi, M. (2009). *Water softening by combination of ultrasound and ion exchange*. Ultrasonics sonochemistry, 16, pp. 356-360.

Eriksson, P. (1998). *Nanofiltartion extends the range of membrane filtration*. Environmental Program, 7, pp. 58–61.

Evans, L.R., & Miller, J.E. (2002). *Sweeping Gas Membrane Desalination Using Commercial Hydrophobic Hollow Fiber Membranes*. Sandia National Labs Report, SAND 2002-0138.

Fujita, Y., Hata, T., Nakamaru, M., Iyo, T., Yoshino, et al. (2005). *A study of boron adsorption onto activated sludge*. Bioresource Technology, 96, pp. 1350–1356.

Gabelich, C.J., Tran, T.D., & Suffet, I.H. (2002). *Electrosorption of inorganic salts from aqueous solution using carbon aerogels*. Environmental Science and Technology, 36(13): 3010–3019.

Galama, A., Daubaras, G., Burheim, O., Rijnaarts, H., & Post, J. (2014). *Ionexchange membranes in seawater applications*. Journal of Membrane Science, 452: pp. 219–228.

Garcia-Aleman, J. (2002). *Mathematical modeling of the pressure-driven performance of McMaster pore-filled membranes*. McMaster University, Hamilton, Ontario, Canada.

García-Soto, M.F., & Camacho, E.M. (2005). *Boron removal from industrial wastewater by ion exchange: an analytical control parameter*. Desalination, 181, pp. 207–216.

Ghaffour, N., Lattemann, S., Missimer, T., Ng, K.C., Sinha, S., & Amy, G. (2014). *Renewable energy-driven innovative energy-efficient desalination technologies*. Applied Energy, 136, pp. 1155–1165.

Global Water Market 2019. (2018). Global Water Intelligence.

McGranahan, G. (2002). *Projected Water Scarcity by 2025*. In: Demand-Side Water Strategies and the Urban Poor.

Greenlee, L. F., Lawler, D. F., Freeman, B. D., Marrot, B., & Moulin, P. (2009). *Reverse osmosis desalination: Water sources, technology, and today's challenges*. Water Resolutions, 43, pp, 2317-2348.

Gude, V.G., & Nirmalakhandan, N. (2009). *Desalination at low temperatures and low pressures*. Desalination, 244, pp. 239–247.

Hamed, O.A. (2005). *Overview of hybrid desalination systems – current status and future prospects*.

Hamouda, S.B., Boubakri, A., Nguyen, Q.T., & Amor, M.B. (2011). *PEBAX membranes for water desalination by pervaporation process*. High Performance Polymers, 23, pp. 170–173.

Han, L., Karthikeyan, K.G., & Gregory, K.B. (2015). *Energy Consumption and Recovery in Capacitive Deionization Using Nanoporous Activated Carbon Electrodes*. Journal of Electrochemical Society, 162(12): E282-E288.

Han, Y., Xu, Z., & Gao, C. (2013). *Ultrathin Graphene Nanofiltration Membrane for Water Purification*. Journal of Advanced Functional Materials, 23: 3693–3700.

Hanaor, D. A. H., Chironi, I., Karatchevtseva, I., Triani, G., & Sorrell, C. C. (2012). S*ingle and Mixed Phase TiO2 Powders Prepared by Excess Hydrolysis of Titanium Alkoxide*. Advances in Applied Ceramics. 111(3): 149–158.

Hemmatifar, A., Palko, J.W., Stadermann, M., & Santiago, J.G. (2016). *Energy breakdown in capacitive deionization*. Water Research, 104, pp. 303-311.

Hench, L. L., & West, J. K. (1990). *The Sol-Gel Process*. Chemical Reviews. 90: pp. 33–72.

Hilder, T.A., Gordon, D., & Chung, S. (2009). *Salt rejection and water transport through boron nitride nanotubes*. Small 5, 2183–2190.

Holst, M.H. (2007). *Solar thermal desalination using the multiple effect humidification method*. In: Solar Desalination for the 21st Century. Springer, Dordrecht.

Holt, J.K., Park, H.G., Wang, Y.M., Stadermann, M., Artyukhin, A.B., et al. (2006). *Fast mass transport through sub-2-nanometer carbon nanotubes*. Science, 312, pp. 1034–1037.

Hummers, W. S. Jr., & Offeman, R. E. (1958). *Preparation of graphitic oxide.* Journal of American Chemical Society, 80, pp. 1339–1339.

Izadpanah, A.A., & Javidnia, A. (2012). *The Ability of a Nanofiltration Membrane to Remove Hardness and Ions from Diluted Seawater*. water, 4, pp. 283–294.

Jarvie, M.E., Hand, D.W., Bhuvendralingam, S., Crittenden, J.C., & Hokanson, D.R. (2005). *Simulating the performance of fixed-bed granular activated carbon adsorbers: Removal of synthetic organic chemicals in the presence of background organic matter*. Water Research, 39(11): 2407–2421.

Jeong, B.H., Hoek, E.M.V., Yan, Y., Subramani, A., Huang, X., et al. (2007). *Interfacial polymerization of thing film nanocomposites: a new concept for reverse osmosis membranes*. Journal of Membrane Science, 294: 1e7.

Jiang, A., Ding, Q., Wang, J., Jiangzhou, S., Cheng, W., & Xing, C. (2014). *Mathematical Modeling and Simulation of SWRO Process Based on Simultaneous Method.* Journal of Applied Mathematics, 908569.

Jong, K.P., In, S.S., & Jong, M.H. (2003). *Application of hybrid technology to the largest desalination plant, Fujairah, UAE*, Proc. IDA World Congress on Desalination and Water Reuse, Bahamas, Sept. 28–Oct. 3, 2003.

Joshi, R.K., Carbone, P., Wang, F.C., Kravets, Su, Y., et al. (2014). *Precise and ultrafast molecular sieving through graphene oxide membranes*. Science, 343, pp. 752–754.

Kabeel, A.E., Hamed, M.H., Omara, Z.M., & Sharshir, S.W. (2013). *Water desalination using a humidification-dehumidification technique – a detailed review*. Nature Resources, 4, pp. 286–305.

Kaufman, Y., Berman, A., & Freger, V. (2010). *Supported lipid bilayer membranes for water purification by reverse osmosis*. *Langmuir*, 26, pp. 7388–7395.

Kelley, T.M., Abulihemu, G., Sanan, T., Neyer, T., Dionysiou, D., & Pressman, J. (2017). *Using Rapid Small Scale Column Testing to Evaluate Granular Activated Carbon Adsorption of Cyanotoxins from Drinking Water*. Submission for AWWA Water Quality Technology Conference, November 13, 2017 at Cincinnati.

Kim, Y.J., Choi, J.H., 2010. *Enhanced desalination efficiency in capacitive deionization with an ion-selective membrane*. Separation and Purification Technology, 71, pp. 70–75.

Kim, T., Gorski, C.A., & Logan, B.E. (2017). *Low Energy Desalination Using Battery Electrode Deionization*. Environmental Science and Technology Letters, 4, pp. 444−449.

Korhonen, J.T., Kettunen, M., Ras, R.H.A., & Ikkala, O. (2011). *Hydrophobic nanocellulose aerogels as floating, sustainable, reusable, and recyclable oil absorbents*. ACS Applied Material Interfaces, 3, pp. 1813–1816.

Köse, T.E., Demiral, H., & Öztürk, N. (2011). *Adsorption of boron from aqueous solutions using activated carbon prepared from olive bagasse.* Desalination & Water Treatment, 29, pp. 110–118.

Kucera, J. (2014). *Desalination: water from water*. New York: John Wiley & Sons.

Kumar, M., Grzelakowski, M., Zilles, J., Clark, M., & Meier, W. (2007). *Highly permeable polymeric membranes based on the incorporation of the functional water channel protein Aquaporin Z*. Proceedings in National Academic Sciences, 104, pp. 20719–20724.

Kuznetsov, Y.P., Kruchinina, E.V., Baklagnia, Y.G., Khripunov, A.K., & Tulupova, O.A. (2007). *Structural and sorption properties of activated carbon modified with iron oxides*. Russian Journal of Applied Chemistry, 80, pp. 790.

Lee, J., Kim, S., Kim, C., & Yoon, J. (2014). *Hybrid capacitive deionization to enhance the desalination performance of capacitive techniques*. Energy Environmental Sciences, 7, pp, 3683-3689.

Lee, S., & Lee, C.H. (2000). *Effect of operating conditions on CaSO4 scale formation mechanism in nanofiltration for water softening*. Water Research, 34: pp. 3854–3866.

Leong, Z.Y., & Yang, H.Y. (2019). *Surface charge enhanced CDI for selective divalent cation removal in water softening applications*. Pillar of Engineering Product Development (EPD), Singapore University of Technology and Design. [Not yet published.]

Leong, Z.Y., Lu, G., & Yang, H.Y. (2019). *Three-dimensional graphene oxide and polyvinyl alcohol composites as structured activated carbons for capacitive desalination*. Desalination, 451(1): 172–181.

Levenstein, R., Hasson, D., & Semiat, R. (1996). *Utilization of the Donan effect for improving electrolyte separation with nanofiltration membranes*. Journal of Membrane Science, 116: 77–92.

Lhassani, A., Rumeau, M., Benjelloun, D., & Pontie, M. (2001). *Selective Demineralization of Water by Nanofiltration Application to the Defluorination of Brackish Water*. Water Resource, 35(13): 3260–3264.

Li, H., Pan, L., Nie, C., Sun, Z., et al. (2012). *Reduced graphene oxide and activated carbon composites for capacitive deionization*. Journal of Materials Chemistry, 22(31): 15556-15561.

Li, D.F., & Yeo, W. (2011). *A Survey of Seawater Desalination in Asia Today*. In: *Measures to the Global Environment Problems* (*Commentary*). Bulletin on Social and Sea Water Sciences, Japan, 65, pp. 10–15.

Li, N., An, J., Wang, X., Ren, Z.J., et al. (2017). Resin-enhanced rolling activated carbon electrode for efficient capacitive deionization. Desalination, 419: pp. 20-28.

Ludwig, H. (2009). *Energy Consumption of Seawater Reverse Osmosis: Expectations and Reality for State-of-the-Art Technology*, IDA World Congress, Dubai, UAE.

Macoun, R.G. (1998). *The mechanisms of ionic rejection in nanofiltration*. University of New South Wales, Sydney.

Malaeb, L., & Ayoub, G.M. (2011). *Reverse osmosis technology for water treatment: state of the art review*. Desalination, 267, pp. 1-8.

Mei, X., Meng, X., & Wu, F. (2015). *Hydrothermal method for the production of reduced graphene-oxide*. Physica E, 68, pp. 81–86.

Al-Mutaz, I.S. (1996). *A comparative study of RO and MSF desalination plants*. Desalination, 106(1–3): 99–106.

Nable, R.O., Banvelos, G.S., & Paull, J.G. (1997). *Boron toxicity*. Plant Soil, 198, pp. 181–198.

Nair, R.R., Wu, H.A., Jayaram, P.N., Grigorieva, I.V., & Geim, A.K. (2012). *Unimpeded permeate of water through helium-leaktight graphene-based membranes*. Science, 335, pp. 442–443.

Nakagawa, Y., Sabio, M.M., & Reinoso, F.R. (2007). *Modification of the porous structure along the preparation of activated carbon monoliths with* H_3PO_4 *and* $ZnCl_2$. Microporous and Mesoporous Materials, 103, pp. 29–34.

NanoH2O, Inc. (2011). *Qfx SW 400 ES SWRO Element Data Sheet*. Retrieved February 2, 2019, from http://www.lg-nanoh2o.com/products/qfx-sw-400-es.

Narayan, G.P., Sharqawy, M.H., Summers, E.K., Lienhard, J.H., et al. (2009). *The potential of solar-driven humidification-dehumidification desalination for small- scale decentralized water production*. Renewable and Sustainable Energy Reviews, 14(4): 1187–1201.

Narayan, G.P., Sharqaqy, M.H., Lienhard, J.H., & Zubair, S.M. (2010). *Thermodynamic analysis of humidification dehumidification desalination cycles*. Desalination Water Treatment, 16, pp. 339–353.

NEWater: The 3rd National Tap. (2018). pub.gov.sg. Retrieved April 17, 2019, from https://www.pub.gov.sg/watersupply/fournationaltaps/newater.

Ng, K.C., Thu, K., Kim, Y., Chakraborty, A., & Amy, G. (2013). *Adsorption desalination: an emerging low-cost thermal desalination method*. Desalination, 308, pp. 161–179.

Nielsen, F.H. (1997). *Boron in human and animal nutrition*. Plant Soil, 193, pp. 199–208.

O'Hern, S.C., Boutilier, M.S.H., Idrobo, J.C., Song, Y., Kong, J., et al. (2014). *Selective ionic transport through tunable subnanometer pores in single-layer graphene membranes*. Nano Letters, 14, pp. 1234–1241.

Oren, Y. (2008). *Capacitive deionization (CDI) for desalination and water treatment—past, present and future* (a review). Desalination, 228, pp. 10-29.

Otowa, T., Tanibata, R., & Itoh, M. (1993). *Production and Adsorption Characteristics of MAXSORB: High Surface Area Active Carbon*. Gas Separation and Purification, 7, pp. 241–245.

Otowa, T., Nojima, Y., & Itoh, M. (1994). In Extended Abstracts ‘Carbon '94', Granada, Spain: Spanish Carbon Group, pp. 808-809.

Otowa, T., Nojima, T., & Miyazaki, T. (1997). *Development of KOH Activated High Surface Area Carbon and Its Application to Drinking Water Purification*. Carbon, 35(9): 1315–1319.

Park, M., Park, J., Lee, E., Khim, J., & Cho, J. (2016). *Smart water grid: desalination water management platform*. Desalination and Water Treatment, 57, pp. 20661-20670.

Paulchamy, B., Arthi, G., & Lignesh, B.D. (2015). *A Simple Approach to Stepwise Synthesis of Graphene Oxide Nanomaterial*. Journal of Nanomedicine and Nanotechnology, 6: 253.

Pei, S.F., & Cheng, H.M. (2012). *The Reduction of Graphene-Oxide*. Carbon, 50, pp. 3210–3228.

Pendergast, M.M., & Hoek, E.M.V. (2011). *A review of water treatment membrane nanotechnologies*. Energy and Environmental Science, 4, pp. 1946–1971.

Porada, S., Weinstein, L, Dash, R., van der Wal, A., Bryjak, M., Gogotsi, Y., & Biesheuvel, P.M. (2012). *Water Desalination Using Capacitive Deionization with Microporous Carbon Electrodes*. ACS Applied Materials and Interfaces, 4, pp. 1194–1199.

Puyol, D. (2009), November. APP — Aguas de Ponta Preta company Technical Department — Personal communication.

Al-Qodah, Z., & Shawabkah, R. (2009). *Production and Characterization of Granular Activated Carbon from Activated Sludge*. Brazilian Journal of Chemical Engineering, 26(1): 127–136.

Raman, L.P., Cheryan, M., & Rajagopalan, N. (1994). *Consider nanofiltration for membrane separation*. Chemical Engineering Program, 90, pp. 68–74.

Radjenović, J., Matošović, M., Mijatović, I., Petrović, M., & Barcelo, D. (2008). *Membrane Bioreactor (MBR) as an Advanced Wastewater Treatment Technology*. In: Handbook of Environmental Chemistry, Vol. 5, Part S/2: pp. 37– 101.

Rattier, M., Reungoat, J., Gernjak, W., & Keller, J. (2012). *Organic Micropollutant Removal by Biological Activated Carbon Filtration: A Review*. Urban Water Security Research Alliance, 53: i–38.

Rovel, J.M., Mazounie, P., & Sanz, M.A. (2003). *Description of the largest SWRO ever built,* Proc. IDA World Congress on Desalination and Water Reuse, Bahamas, Sept. 28–Oct. 3, 2003.

Royan, F. (2012, May 15). *Sustainable Water Treatment Technologies in the 2020 Global Water Market — Investor Briefing: Water- An attractive investor opportunity*. Global Environment (Water) Markets.

Royan, F. (2016, October 13). *Global Water Market Outlook Water & Wastewater Treatment Market European Network Rehabilitation Market*. Global Environment & Water Practice Energy & Environment, British Water International Forum Meeting.

Sakurai, K., & Mizusawa, M. (2010). *X-ray Diffraction Imaging of Anatase and Rutile*. Analytical Chemistry, 82(9): 3519–3522.

Sarkar, S., & Sengupta, A.K. (2008). *A new hybrid ion exchange–nanofiltration (HIX–NF) separation process for energy-efficient desalination: process concept and laboratory evaluation*. Journal of Membrane Science, 324, pp. 76–84.

Sarkar, S., & Sengupta, A.K. (2009). *A hybrid ion Exchange–Nanofiltration (HIX– NF) Process for Energy Efficient Desalination of Brackish/Seawater*. Journal of Membrane Science, 9, pp. 369–377.

Sengupta, P. (2013). *Potential health Impacts of Hard Water*. International Journal of Preventive Medicine, 4(8): 866–875.

Al-Shayji, K.A., & Liu, Y.A. (2002). *Predictive Modeling of Large-Scale Commercial Water Desalination Plants: Data-Based Neural Network and Model-Based Process Simulation*. Industrial & Engineering Chemistry Research , 41(25): 6460-6474.

Shon, H.K., Phuntsho, S., Chaudhary, D.S., Vigneswaran, S., & Cho, J. (2013). *Nanofiltration for water and wastewater treatment — a mini review*. Drinking Water Engineering and Science, 6: 47–53.

Energy-efficient Seawater Desalination. (2009). Siemens. Retrieved November 25, 2014, from http://www.siemens.com/press/en/presspicture/?press./en/presspicture/pictures-photonews/2009/pn200906/pn200906-02.htm.

Song, L., Hu, J.Y., One, S.L., Ng, W.J., Elimelech, M., & Wilf, M. (2003). *Emergence of thermodynamic restriction and its implications for full-scale reverse osmosis processes*. Desalination, 144, pp. 213–228.

Stover, R.L. (2009). *Evolution of energy consumption in seawater reverse osmosis.* Desalination andWater Reuse, 19(2): 27–30.

Stover, R.L. (2013). *Permeate recovery and flux maximization in semi-batch reverse osmosis*. In: Proceedings of the American Water Works Association (AWWA) and American Membrane Technology Association (AMTA) Membrane Technology Conference, February 25–28, San Antonio, Texas.

Stover, R.L., & Efraty, N. (2011). *Record low energy consumption with closed circuit desalination*. In: International Desalination Association (IDA) World Congress — Perth Convention and Exhibition Center (PCEC), Perth, Western Australia, September 4–9, 2011.

Subramani, A., & Jacangelo, J.G. (2015). *Emerging desalination technologies for water treatment: A critical review*. Water Research, 75: 164–187.

Subramani, A., Voutchkov, N., & Jacangelo, J.G. (2014). *Desalination energy minimization using thin film nanocomposite membranes*. Desalination, 350, pp. 35–43.

Sui, H., Han, B.G., Lee, J.K., Walian, P., & Jap, B.K. (2001). *Structural basis of water specific transport through the AQP1 water channel*. Nature, 414, pp. 872– 878.

Tavani, L. (1971). *Desalination Process by Ion Exchange*. US3618589A.

Qin, M., Deshmukh, A., Epsztein, R., Patel, S.K., Owoseni, O.M., et al. (2019). *Comparison of energy consumption in desalination by capacitive deionization and reverse osmosis*. Desalination, 455, pp. 100–114.

Qu, Y., Campbell, P.G., Gu, L., Knipe, J.M., Dzenitis, E., et al. (2016). *Energy consumption analysis of constant voltage and constant current operation in capacitive deionization*. Desalination, 400: pp. 18–24.

U. Water, United Nations Educational Scientific and Cultural Organization, Paris, 2009.

Urairi, M., Tsuru, T. Nakao, S.I., & Kimura, S. (1992). *Bipolar reverse osmosis membrane for separating mono- and divalent ions*. Journal of membrane science, 70, pp. 153-162.

Voutchkov, N. (2018). *Energy use for membrane seawater desalination – current status and trends*. Desalination, 431, pp. 2–14.

Wang, F., He, X., Sun, L., Chen, J., Wang, X., et al. (2018). *Engineering an N- doped TiO2@N-doped C butterfly-like nanostructure with long-lived photogenerated carriers for efficient photocatalytic selective amine oxidation*. Journal of Materials Chemistry A, 6, pp. 2091–2099.

Water Desalination by the Numbers. (2011). International Desalination Association. Retrieved , from http://idadesal.org/desalination-101/desalination-by-the-numbers/.

Welgemoed, T.J. (2005). *Capacitive Deionization Technology: Development and Evaluation of an Industrial Prototype System*. University of Pretoria. Dissertation.

World Health Organization. (2011). *Hardness in Drinking-water: Background document for development of WHO Guidelines for Drinking-water Quality*. WHO/HSE/WSH/10.01/10/Rev/1 .

Xing, B., Shi, C., Zhang, C., Yi, G., Chen, L., et al. (2016). *Preparation of TiO2/Activated Carbon Composites for Photocatalytic Degradation of RhB under UV Light Irradiation*. Journal of Nanomaterials, 8393648.

Zhang, C., Long, D., Xing, B., Qi, W., Zhang, R., et al. (2008). *The superior electrochemical performance of oxygen-rich activated carbons prepared from bituminous coal*. Electrochemistry, 10(11): 1809–1811.

Zhao, R., Biesheuvel, P.M., & van der Wal, A. (2012). *Energy consumption and constant current operation in membrane capacitive deionization*. Energy Environmental Science, 5, 9520.

Zhao, R., Porada, S., Biesheuvel, P., & Van der Wal, A. (2013). *Energy consumption in membrane capacitive deionization for different water recoveries and flow rates, and comparison with reverse osmosis.* Desalination, 330, pp. 35-41.

Zheng, X., Peng, Y., Yang, Y., Chen, J., Tian, H., et al. (2017). *Hydrothermal reduction of graphene-oxide; effect on surface-enhanced Raman scattering*. Journal of Raman spectroscopy, 48, pp. 97–103.

Zhou, Y., Bao, Q.L., Tang, L.A.L., Zhong, Y.L., & Loh, K.P. (2009). *Hydrothermal Dehydration for the "Green" Reduction of Exfoliated Graphene Oxide to Graphene and Demonstration of Tunable Optical Limiting Properties*. Journal of American Chemical Society, 21(13): 2950–2956.

Zhou, D., Zhu, L., Fu, Y., Zhu, M., & Xue, L. (2015). *Development of lower cost seawater desalination processes using nano filtration technologies*. Desalination, 376, pp. 109–116.

Zwijnenberg, H.J., Koops, G.H., & Wessling, M. (2005). *Solar driven cost membrane pervaporation for desalination processes*. Journal of Membrane Sciences, 250, pp. 235–246.